University of Southern Queensland

Faculty of Engineering and Surveying

Investigation on the Fatigue Behaviour of Pultruded Fibre Composites

A dissertation submitted by

Alan Owen Taylor

In fulfilment of the requirements of

Courses ENG4111 and 4112 Research Project

Towards the degree of

Bachelor of Engineering (Civil)

Submitted: October, 2009

Abstract

Fibre Composites existence in civil infrastructure and transportation is relatively new. Originally developed for aerospace, defence force and marine industries, composite materials did not make an appearance into large civil structures until the first legal road bridge was constructed in 2002. They have many advantages over conventional materials such as improved durability and high strength to weight ratio just to name a few. The behaviour of pultruded fibre composites has been studied to help the design engineer to better understand the long term performance of composite structures.

This research project seeks to investigate the fatigue behaviour of pultruded fibre composites to help develop the fatigue curve or better known as the fatigue life of a material. Firstly a literature review was undertaken to help better understand the theory behind fibre composites and secondly a series of small scale (coupons) and large scale (Composite bridge girder) testing was done to prove these theories. This project also aimed to determine whether small scale testing can predict the fatigue life of large scale composite structures.

Fatigue testing is a lengthy process with many researchers spending years just to develop one fatigue curve. Testing a particular sample to one million cycles at one hertz for example takes roughly 12 days to complete, and this does not including setup time. It may seem like the results obtained throughout this research project are quite small, however that one fatigue curve that is obtained is extremely important for the long term performance of pultruded fibre composites.

By applying a prediction model to the small scale experimental data, the fatigue curve was developed. Initial results were not quite what were expected, however they did provide an insight into the fatigue performance of coupon testing as this was something that had never been done before on these products. There are minor flaws in the coupon testing, however these did not become apparent until final tests were completed. Further research into the use of coupons for fatigue testing purposes would be recommended. The composite bridge girder on the other hand showed extremely satisfying results considering it was tested at more than double the serviceability load specified by the Queensland Department of Main Roads.

University of Southern Queensland

Faculty of Engineering and Surveying

ENG4111 & ENG4112 *Research Project*

Limitations of Use

The Council of the University of Southern Queensland, its Faculty of Engineering and Surveying, and the staff of the University of Southern Queensland, do not accept any responsibility for the truth, accuracy of completeness of material contained within or associated with this dissertation.

Persons using all or any part of this material do so at their own risk, and not at the risk of the Council of the University of Southern Queensland, its Faculty of Engineering and Surveying or the staff of the University of Southern Queensland.

This dissertation reports an educational exercise and has no purpose of validity beyond this exercise. The sole purpose of the course pair entitled "Research Project" is to contribute to the overall education within the student's chosen degree program. This document, the associated hardware, software, drawings, and other material set out in the associated appendices should not be used for any other purpose: if they are so used, it is entirely at the risk of the user.

Prof Frank Bullen
Dean
Faculty of Engineering and Surveying

Certification

I certify that the ideas, designs and experimental work, results, analyses and conclusions set out in this dissertation are entirely my own effort, except where otherwise indicated and acknowledged.

I further certify that the work is original and has not been previously submitted for assessment in any other course or institution, except where specifically stated.

Alan Owen Taylor

Student Number: 0050057217

_____

Signature

_____

Date

Acknowledgements

I would like to thank my supervisor Associate Professor Thiru Aravinthan for his continued support throughout this research project. I would also like to thank Michael Kemp from Wagners Fibre Composite Technologies for providing me with the products industry support that I needed. I would also like to thank the production staff at Wagners Composite Fibres Technologies for allowing me to use their work shop for preparation of samples. I would also like to thank Mohan Trada and Wayne Crowell for all their help in testing and preparation. A final thank you goes to Associate Professor Jayantha Epaarachchi for assisting me with his knowledge on fatigue of fibre composites

Contents

List of Figures

List of Tables

Chapter 1: Introduction

1.1 Project Background

Fibre Composites (FC) existence in civil infrastructure and transportation is relatively new. Originally developed for aerospace, defence force and marine industries, FC material did not make an appearance into large civil structures until the first legal road bridge was constructed in 2002. They posses many advantages over conventional materials (such as steel, concrete or wood) including improved durability, high strength to weight ratio, rust proof and costs as a whole-life basis are often considered to be lower [Wagners, 2009].

An area of research that has not been thoroughly tested is the effects of fatigue on FC superstructures. Fatigue is an important characteristic a design engineer must consider throughout the design process, particularly in the design of road and railway bridges. Australian Standards defines fatigue as damage caused by repeated fluctuations of stress leading to gradual cracking of a structural element. In simple terms, the life-span of a material is continually reduced when subject to a stress cycle of any magnitude.

The broad aim of this project was to explore the effects of fatigue behaviour on pultruded Fibre Reinforced Plastics (FRP) through a series of small scale (coupon) and large scale (composite beam) tests and to make a conclusion on the relationship between the two testing methodologies. Research and testing has been undertaken under the guidance of both the University of Southern Queensland's (USQ) Centre of Excellence in Engineered Fibre Composites (CEEFC) and Wagners Composite Fibres Technologies (WCFT). Formally known as Fibre Composite Design and Development (FCDD), CEEFC is one of the leading research centres in FC in the world today. It has an international reputation for research and development for the application of FC in civil infrastructure. The team at CEEFC includes a variety of multi-disciplinary staff who specialise from civil to polymers engineering. CEEFC was involved in the development of Australia's first FC Bridge in junction with industry partners. Figure 1 below is a 100 by 100 pultruded box section that is manufactured by WCFT.

Figure 1 - Pultruded Fibre Composite

WCFT has been at the forefront in development and manufacturing of composite infrastructure using the pultrusion FC manufacturing process. They are credited with manufacturing and installing the world's first composite road bridge in a public road network. WCFT has successfully applied the composite fibre technology to a number of products including road bridges, electrical cross arms and boardwalks.

1.2 Research Aim and Objectives

The research testing methodologies and procedures were based on the following Aims and Objectives. Firstly the projects two major aims were to:

1. Investigate the fatigue behaviour of pultruded Fibre Reinforced Plastics (FRP); and
2. Perform small scale tests (coupons) to extrapolate the same results as for large scale beams.

Secondly, to successfully complete the major research aims the following objectives had to of been met:

1. Research background information into the theory of fatigue life for steel, FRP, and existing fatigue studies.
2. Analysis of Wagners 9.7 m composite bridge girder which has been fatigue tested at USQ facilities.

3. Develop a testing plan including placement of instrumentation, static and live loading of the coupons.
4. Fatigue test pultruded coupons for S-N curves.
5. Analysis of S-N curves from pultruded FRP sections.
6. Determine whether or not small scale tests (coupon) can be used as a means of predicting the fatigue life of large scale beams.

As time permits the following two objects will be met:

7. Develop design guidelines considering fatigue behaviour.
8. Fatigue test glue line coupons.

1.3 Structure of Dissertation

Chapter 2: Literature Review, appraises the available literature relating to this project. This is achieved by exploring the elements that make up pultruded FC, the manufacturing pultrusion process, civil applications that are used in the industry today and a brief look into fatigue studies that have been undertaken on FC. The chapter also looks at the theory behind the fatigue curve, or commonly referred to as the S-N curve (Stress versus Cycles curve).

Chapter 3: Testing Methodology gives details on the methodologies used to explore the fatigue properties of pultruded FC. This has been achieved by developing testing plans to determine the tensile and fatigue properties of coupons as well as developing a testing plan to determine the fatigue performance of the composite bridge girder.

Chapter 4: Results & Discussions presents the results found from the testing methodologies and any observations that have been made throughout testing. The chapter also discusses the accuracy of the results obtained and provides a starting point the analysis and discussions.

Chapter 5: Analysis & Discussions investigates on the results from fatigue tested coupons by applying a prediction model to the given experimental data. The prediction model helps determine the fatigue performance of FC through the use of theory and experimental results. This chapter makes conclusions on whether or not

small scale testing can be used as a means of predicting the fatigue life of large scale FC structures.

Chapter 6: Conclusion summarises the discussions and results found from the literature and testing. This chapter answers the major aims and objectives which have been outlined in Chapter 1 and makes any conclusions and recommendations as a result of these outcomes.

1.4 Summary

As stated earlier this project has endeavoured to investigate the fatigue behaviour of pultruded fibre composites as shown in the coming chapters. Fatigue design is an important characteristic of structural design. It gives guidance to a design engineer to help prevent structural failure as a result of fatigue. Design standards are in place for the design of steel, concrete and wood structures, however no such codes exist for the design of FC materials in Australia, thus showing the results from this study are extremely important.

Chapter 2: Literature Review

2.1 Introduction

At a fraction of the weight of traditional building materials, a fibre composite material can be designed to carry a load up to six times higher than steel or concrete. FC material is generally made from polymers (plastics) which can be reinforced with carbon, glass and/or aramid (Kevlar) type fibres. They are generally easy to assemble, flexible and durable, and as a result are increasingly considered for use in government and industry infrastructure projects [Wagners, 2009]. Some of the major advantages FC have over conventional materials include the following:

- High tensile strength
- Heat resistance
- Thermal Behaviour
- Chemical Resistance
- Moisture resistance
- Fire resistance
- Electrical resistance

As stated in Chapter 1, this chapter reviews the available literature relating to this project, which includes the theory behind the core materials of pultruded FC, the pultrusion manufacturing process, civil applications and fatigue studies that have been undertaken on FC. This chapter also looks at the theory behind the fatigue curve, or commonly referred to as the S-N curve (Stress versus Cycles curve).

2.2 Pultrusion Composite Materials

2.2.1 Fibre Reinforcement

A pultruded FC section consists of two main elements, a fibre reinforcement and polymer matrix. The fibre reinforcement determines the core structural properties such as tensile strength and stiffness and is the primary load carrying element of a composite section. It is therefore important to select the correct fibre reinforcement for the design task. Fibre reinforcement also affects the density, compressive strength, modulus, costs and most importantly fatigue performance. Some of the

main fibre reinforcement types used in civil infrastructure includes glass, carbon and aramid type reinforcement. Figure 2 below shows what glass fibre looks like before it is pultruded into a composite section.

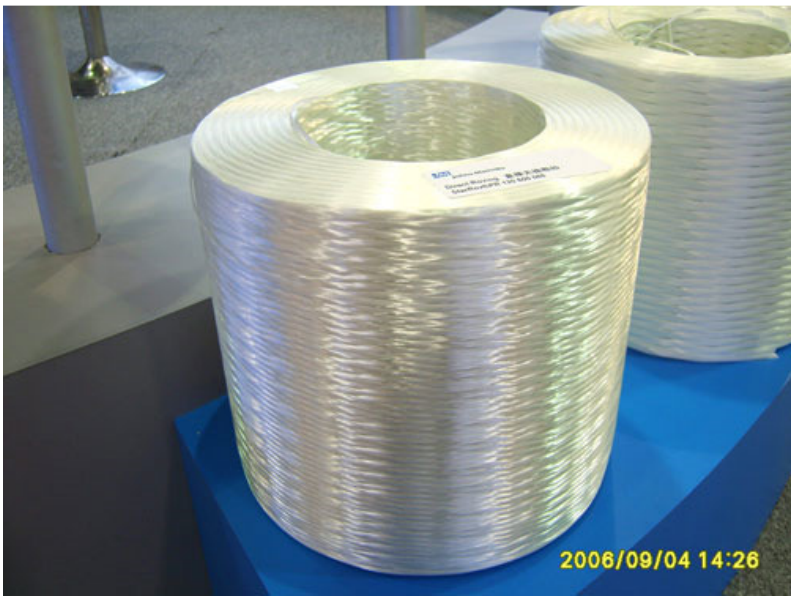

Source: http://www.made-in-china.com/image/2f0j00cCztvaeBaVkEM/Glass-Fibre-Assembled-Panel-Roving-E-Glass-.jpg

Figure 2 - Glass Fibre Strands

Glass is the most common fibre reinforcement available, which can be credited to the low costs and flexibility of its use. They have been used since the 1940's and have a good history in the composite industry. Glass fibres can be split into four common types, E, S2, A and C-glass, where E-glass is the most common. Each different type of glass reinforcement has its own advantages and disadvantages.

E-glass and S2-glass reinforcement are widely used in structural applications whereas A-glass and C-glass are used to create a surface barrier layers over a structural composites due to their chemical resistance properties. E-glass has high electrical resistance, thus making them perfect for electrical cross arms. S2-glass is a more expensive alternative to E-glass, but has stronger structural properties making it more reliable in structural applications.

Due to glass fibre reinforcement having a low modulus of elasticity (approximately equal to the modulus of elasticity of concrete), carbon fibre reinforcement is preferred for primary structural elements. The modulus of elasticity of carbon can rival that of steel. It also has excellent long term performance where as glass fibres do not. However the costs are significantly higher than glass fibres with carbon

costing up to $1000/kg, where as glass fibres will cost around $10/kg [USQ, 2008]. Carbon tends to find it difficult to compete with traditional materials due to its high costs.

The third and final fibre reinforcement which is not widely known is Aramid. Aramid fibres are extremely tough and have a high impact performance when compared to carbon and glass fibres [USQ, 2008]. They are mainly used as a ballistic protection application such as body armour for defence forces (Army, Police, etc). Aramid fibre reinforcement has the potential to be used in civil applications such as car barriers on the side of road bridges because of their high impact performance.

2.2.2 Resin

As described above, fibre reinforcement has strong strength and stiffness properties; however it has little or no compressive or shear properties. The polymer matrix (commonly referred to as resin) binds the fibre reinforcements together to form a single cohesive structural system [Young, 1993]. This transfers the loads between fibres so that it can act as a single material system with stronger compressive and shear prosperities. Figure 3below shows a typical epoxy vinyl ester resin.

Source: http://img.directindustry.com/images_di/photo-g/fire-retardant-novolac-epoxy-vinyl-ester-resin-329843.jpg

Figure 3 – Epoxy Vinyl Ester Resin

Resins possess many different properties and it is important for the designer to select the correct resin for the design task. For civil infrastructure there are three main thermosetting resins which are:

1. Epoxy,
2. polyester, and
3. Vinyl ester.

As the same for fibre reinforcement, each resin has different characteristics which include curing temperatures, chemical resistance or costs per kilogram. An epoxy resin is widely used in a high performance application because of its increased strength and excellent structural properties, thus making it the better choice for primary structural elements. However the costs associated with an epoxy resin are much greater than polyester or vinyl ester resins.

Polyester resins are cost effective, however their poor performance with carbon fibre, low toughness, and low strain characteristics deter them from primary structural applications. Vinyl esters have the best of both worlds. They are low in costs compared to epoxy resins and possess stronger performance characteristics than polyester resins. However vinyl esters also have a poor performance with carbon and low strain characteristics. Hence vinyl esters resins are better suited to secondary structural applications.

2.3 Pultrusion Composite Manufacturing

A pultruded FC has continuous fibre reinforcements. The FC can be continually manufactured to any desired length. The manufacturing process usually requires less labour and is a time efficient process, which usually involves four simple steps:

1. Placement of fibre reinforcement,
2. Resin injection tank,
3. pultrusion die, and
4. pulling mechanism and cut-off saw.

The first of these four steps is the determination of fibre reinforcement. Type of reinforcement can consist of glass, carbon, aramid and other fibre types as described previously. This stage requires a large storage area as the roving racks containing the fibre stands are large in size. The fibres are weaved through an alignment card (prevents twisting and tangling of the fibres), which are transferred to the resin injection tank.

The resin injection tank injects the resin into the fibres and as described above is what holds the fibres together to form the compressive and shear properties. The type of resin can vary depending on the design purpose.

The third step is considered to be the most important stage. It involves passing the fibres through a mechanical die and heater. The purpose of the die is to shape the fibre composite, maintain fibre alignment and compress loose fibres to the final design shape. The fibres leave the die as cured whole section.

The fourth and final stage is where the fibre cross section is pulled and cut off. The pulling mechanism is what drives the entire systems and pulls the fibres through the roving racks, resin injection tank and die. The fibre cross section continues to cure between the die and pulling mechanism. After the pulling mechanism a cut off saw can cut the fibre cross section to any desired length. The saw is usually a radial saw and is mounted on a bench that moves with the pultrusion so that a clean cut is evident. The entire process can be summarised by a basic schematic as shown in Figure 4 below.

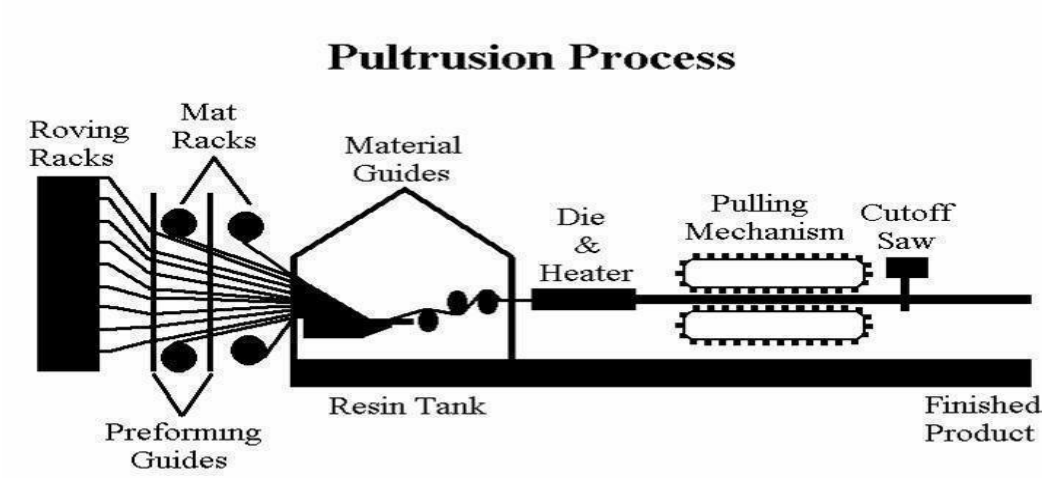

Source: http://www.ultrafiberglass.com/pultrusion%20process.jpg

Figure 4 - Basic Pultrusion Process

2.4 Civil Applications of Pultruded Fibre Composites

2.4.1 Composite Bridges

Pultruded fibre composites can be designed in a way where they can be used as a bridge superstructure. A composite bridge deck is made up of three major elements, firstly the deck or compression flange is made from concrete, secondly a collection

of hollowed out square pultrusions are bonded together to form the web and thirdly a solid pultruded FC section forms the tensile flange. Special adhesives are used to bond each of these elements together to form a box section which acts as deck unit. Multiple deck units are placed next to each other on a concrete substructure to form a bridge as shown in Figure 5.

Figure 5 - Wagners Composite Bridge Deck

Composite bridge decks are designed so that they replicate the behaviour of concrete bridges. Composite bridge decks weigh approximately one third of a conventional concrete bridge of comparable size [Wagners, 2009]. Composite decks contain no corrodible materials, thus making the decks an appropriate choice for high corrosive areas such as the cost line. This can reduce the overall maintenance costs for the life time of the structure.

2.4.2 Electrical Cross Arms

Composite electrical cross arms (shown in Figure 6) are designed to completely replace existing wooden cross arms. They possess many advantages such as reduced pole top fires, lightweight, corrosion resistance, low maintenance and reduced strain on the operator during installation.

Figure 6 - Wagners Composite Cross Arm

Composite electrical cross arms can be produced continuously over 24 hours and anywhere up to a 1000 a week can be produced, depending on the pultrusion machine capabilities. The life time costs of composite cross arms are significantly less than the conventional wooden cross arms.

2.4.3 Bridge Girders

Composite bridge girders have been designed so that they meet the requirements of the Queensland Department of Main Roads (QMR). They have been designed to replicate the strength and stiffness of an equivalent 19 inch diameter round timber girder. Composite bridge girders possess the same characteristics as for bridge decks and cross arms. Their main purpose is to replace existing deteriorating wooden girders. Maintenance costs are expected to be lower and the life spans are expected to be longer. Weight is much lower with a nine metre composite bridge girder weighing only 650 kilograms [Wagners, 2009].

2.4.4 Board Walks

Composite board walks follow the same design pattern as conventional boardwalks. They use joists, bearers, stumps and handrails. However, composite board walks don't rot or corrode which is the main problem for wooden board walks. Hardwood timber is also becoming increasingly expensive to obtain and are vulnerable to termite and marine borer attacks. Composite board (shown in Figure 7) walks are extremely versatile, lightweight and environmentally friendly.

Figure 7 - Wagners Composite Board Walks

2.5 Fatigue

2.5.1 Fatigue Theory

The word 'fatigue' was introduced in the 1840's and 1850's to describe failures occurring from repeated stresses. Engineers discovered that if you repeatedly applied and then removed a nominal load to and from a metal (known as a cyclic load), the metal would break after a certain number of load-unload cycles [EPI Inc, 2008]. They described this as a fatigue failure. In civil engineering, fatigue mainly affects structures that are subject to cyclic loading such as bridges, roads and highways. Fatigue can be described as the manifestation of progressive fractures in a solid under cyclic loading [Encyclopaedia Online] and can be classified by the form in which it occurs, whether it is mechanical, creep, thermo-mechanical, corrosion or rolling contact. It can also be classified by the duration of the cyclic load, whether it is low-cycle or high-cycle case. The most common types of fatigue found in civil infrastructure are mechanical and high-cycle fatigues.

Perhaps the most notable civil structure that is most at risk to the effects of fatigue is railway bridges. Fatigue is a major issue affecting safety and quality of service in the railway industry. Fatigue failure in railway bridges can include rails, fixings and sleepers. The contact of steel wheels to steel tracks is also a form of fatigue. The number of cycles a railway bridge reaches in its life time is a lot higher than conventional bridges. High traffic railway bridges can reach anywhere up to 100 million cycles in its lifetime. It is extremely important to study the effects of fatigue on FC structures when considering them for the railway industry.

Fatigue can often be divided into two phases; crack initiation and crack propagation. The first phase, crack initiation is where a crack is formed, usually around an inclusion or other defect. The second phase, crack propagation usually occurs when the crack increases in length with subsequent load cycles. The boundary between the two phases is often very difficult to determine [Paasch et al, 1999]. Engineers also discovered that as the magnitude of the cyclic stress is reduced, a material would survive more cycles before failure. They commonly referred to the number of cycles material could withstand as the fatigue life.

2.5.2 Fatigue Life

Fatigue analysis generally comes under three general methods; stress-life, strain-life and linear-elastic fracture mechanics [Paasch et al, 1999]. These methods are designed to determine the fatigue life of a material or structure. This research project focuses on the method stress-life analysis to develop a fatigue curve. The fatigue stress-life can be defined as the number of stress cycles (N) of a specified character (low-cycle, high-cycle) that a specimen sustains before failure (mechanical, creep, corrosion, etc). It is influenced by a number of factors such as loading, geometry, material, environmental parameters and fabrication-induced residual stresses.

Fatigue is generally represented by an S-N curve, where stress amplitude is plotted against the number of stress cycles a specimen sustains before failure. Put simply, when a specimen is subject to a higher stress, it will sustain smaller cycles before failure. To understand the fatigue behaviour of FC, firstly a brief overview of metal fatigue must be explored.

2.5.3 Metal Fatigue

Metal fatigue has been under study since the early 1840's when the first major impact of failures due to fatigue involved the railway industry. Engineers discovered that railroad axles failed regularly at shoulders [Stephens et al, 2001]. The first systematic fatigue testing was undertaken by a German Engineer August Wöhler whom performed many laboratory fatigue tests under repeated stresses. Wöhler showed clearly that fatigue occurs by crack growth from surface defects until the product can no longer support the applied load. He was able to develop the first S-N curve, also known as Wöhler curve, which helped standardise testing and

certification of iron and steel. A typical S-N curve is represented in Figure 8 shown below.

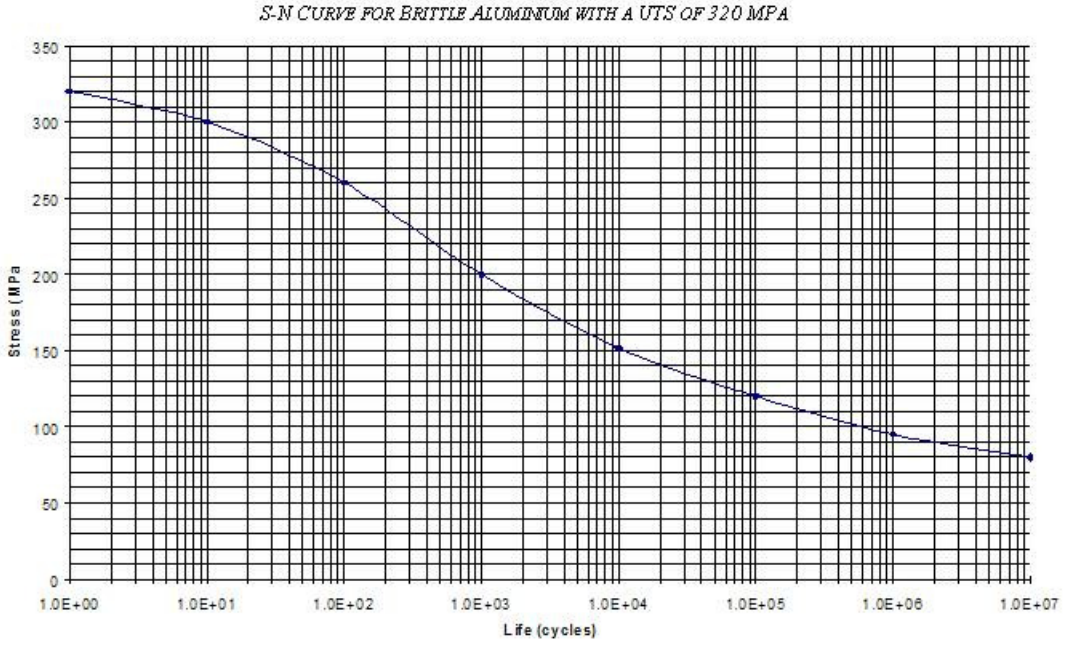

Figure 8 - Typical S-N Curve

It can be seen in Figure 8 that as the stress inflicted in the material reduces the number of cycles before failure increase to a point where the cycles are considered to infinite. The point where the cycles are considered infinite is known as the endurance limit or the constant stress range fatigue limit [Australian Standards, AS4100] and is true for many metal alloys. In general, steel alloys which are subjected to a cyclic stress level below the endurance limit will not fail in fatigue [EPI Inc, 2008]. The Australian Standards suggests that the stress level in which the material reaches five million cycles is considered to be the endurance limit. Different standards around the world suggest a different number of cycles, with most suggesting 10 million cycles. If all stress cycles are below this level then the fatigue life is theoretically infinite. However, if a small percentage, as little as 0.1%, is above the fatigue limit, then stress ranges below the fatigue limit contribute to fatigue damage [Grundy, 2003].

Figure 9 below represents the behaviour of a metal alloy under fatigue. It can be seen that when the stress amplitude S = 50 MPa the number of stress cycles N = 2 million is reached and at 37 MPa, 5 million cycles are reached [Grundy, 2003]. It can also

been in the figure that endurance limit of the material is at 20 MPa, which in this case occurs at 100 million cycles.

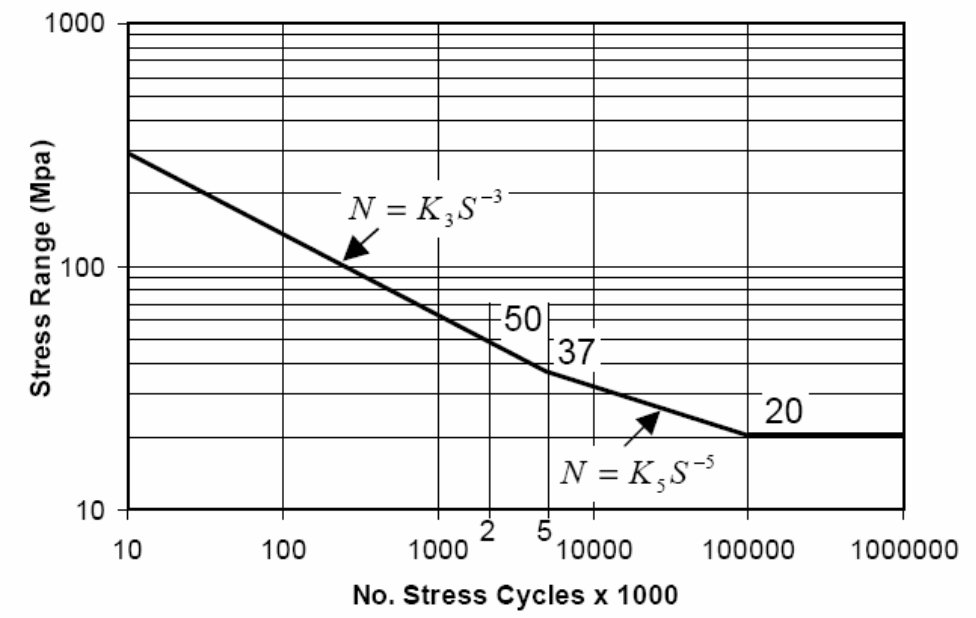

Figure 9 - Typical Design S-N Curve

2.5.4 Fibre Composite Fatigue

The limited test data available suggest that for glass fibre reinforced composites there is no evidence of a fatigue limit at 10 million cycles [Shafeeq, 2006]. FC fatigue failure modes depend on the nature of the loading conditions (whether tensile or compressive) and whether or not the loads have been applied parallel to the fibre reinforcement or at some other angle [R. O. Ritchie, 2003]. Failure modes also depend on the type of fibre reinforcement and configuration used. Composites typically fail as a result of the statistical accumulation of defects, rather than as a result of the statistical distribution of defects or flaws [R. O. Ritchie, 2003].

The fatigue behaviour of FC is considered to be rather different to a metal alloy fatigue, in the sense that FC does not have an endurance limit like most metal alloys. Epaarachchi suggests that a FC material will continually degrade over time and will eventually failure as a result of fatigue. However, further experimental studies into the fatigue behaviour at low-stress, high-cycle cases need to be properly investigated to prove this theory.

The fatigue behaviour of composites has shown to be highly dependent on the stress ratio, R, and the frequency of applied cyclic loading, f, [Epaarachchi et al, 2003].

Mandel and Meir have discussed the effects of *R* on the fatigue life of composites and have shown that for a given maximum stress in a tension-tension case, the fatigue life of the composite increases with increasing magnitude of *R*. The stress ratio, *R*, is equal to the relationship between minimum and maximum stress applied to a sample during testing. Put simply, if a sample was subject to a minimum stress of 4 MPa and a maximum stress of 40 MPa, then the stress ratio would be 0.1 (minimum/maximum stress). Ideally for testing tension-tension cases, an *R* value of *0.1* is preferred.

Due to the visco-elastic nature of matrix materials, it has been found that by increasing the load frequency most of the polymers and composites shown extended fatigue life, provided that the temperature of the sample remains unchanged [Epaarachchi et al, 2003]. Figure 10 below adequately addresses the effects of frequency on FC materials.

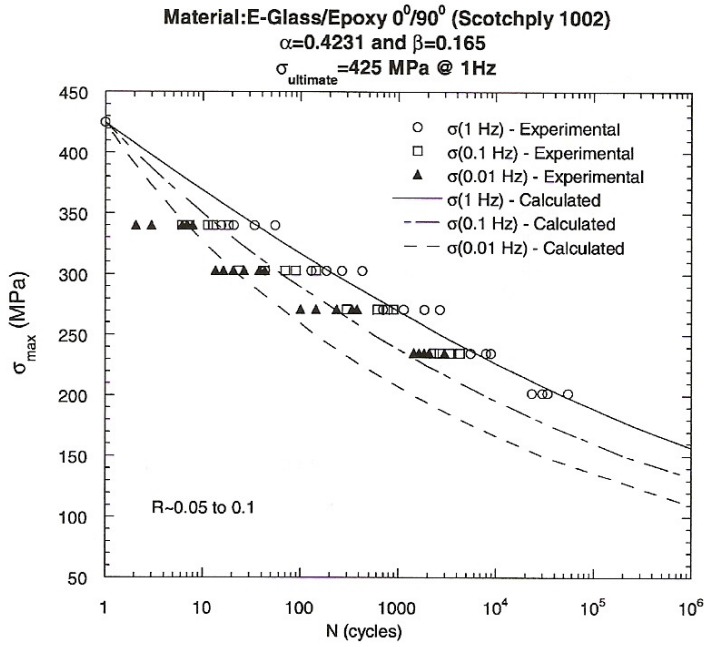

Source: Epaarachchi et al, 2003

Figure 10 - Effects of Frequency

The effects of stress ratios and load frequencies will be further discussed in the coming chapters. There many variables a design engineer must consider when using FC. To make things more difficult no such Australian Standards have been developed for the design of FC structures, with the exception of the design standard

available for the determination of tensile properties of fibre reinforced polymers (AS 1145.4, AS 1145.5, 2001).

2.6 Summary

This chapter addresses the many advantages of using FC material as a replacement to conventional materials such as steel, concrete or wood. It gave a brief look into the makeup of FC as well as the manufacturing process of pultruded FC. Due to a confidentiality agreement, the true material properties such as fibre layout, fibre to resin ratio and manufacturing process cannot be properly disclosed. For this reason alone, the basic material properties that make FC have been only explored. An overview of the general pultrusion process and civil applications where pultruded FC are being used in the industry today have also been discussed.

This chapter also addressed the theories behind fatigue and the concept of fatigue life on metals and FC. A brief overview of metal fatigue was discussed which was compared to the theories behind FC fatigue. It was discussed that the major difference between metal and composite fatigue was the absence of the endurance limit with in FC fatigue life. However it was also noted that further experimental studies needed to be performed before any such judgements could be made. The theories outlined in this chapter have been explored through experimentation in the coming chapters.

Chapter 3: Testing Methodology

3.1 Introduction

The design of pultruded fibre composite structures is based upon the characteristic material properties of their components. This chapter outlines the testing performed to evaluate the tensile and fatigue properties, and the methodologies used to interpret the test results. Results from testing are showing the in following chapter, Chapter 4: Results and Discussions.

3.2 Static Coupon Testing (Tensile)

3.2.1 Overview

A lot can be learnt from tensile testing. As the material is subject to a tension or pulling force a smooth curve is produced which can tell a number of different properties (as shown in Figure 11 below). The point of maximum stress is the most important aspect and is typically called its Ultimate Tensile Strength (UTS or σ_{ult}). The purpose of performing tensile tests on the FC samples was to determine the ultimate characteristic tensile strength of the material. This will inevitably form the starting point for all dynamic coupons testing which will be discussed in the coming sections.

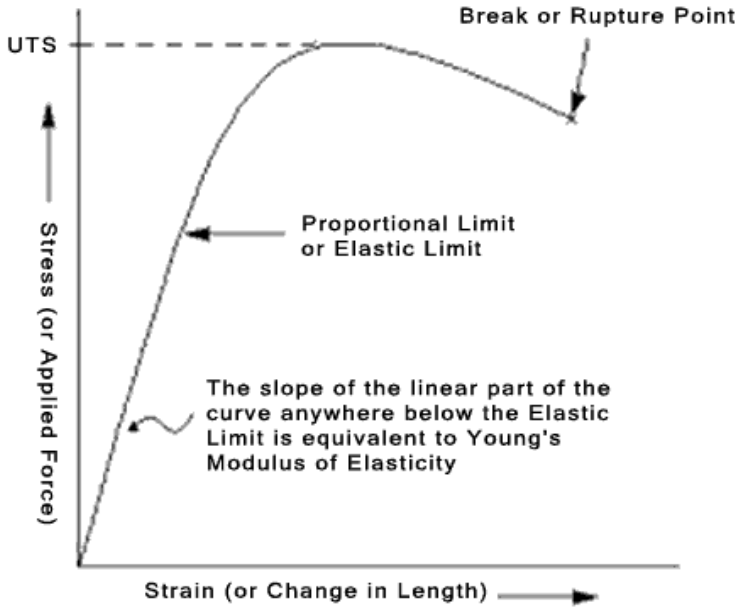

Figure 11 - Typical Stress vs. Strain

From a typical stress-strain curve (as shown above), material properties such as Young's Modulus, Ultimate Tensile Strength and the breaking or rupture point are shown. Tensile testing has been in practice since the late 1800's and as a result a standardised testing procedure has been put in place.

3.2.2 General Method

Australian Standards *AS1145.4-2004: Determination of tensile properties of plastics materials* was used to determine the tensile properties of the pultruded FC coupons. Testing Standard *ASTM D3039: Standard Test Method for Tensile Properties of Polymer Matrix Composite Materials* was the test method which was followed in order to determine these properties. The coupons were sourced from 100 x 100 x 5 Circumferentially Wound Pultrusions. Typically a FC section has different structural properties in the lengthwise and cross wise directions. Shown in Figure 12 is the difference between lengthwise and cross wise coupons.

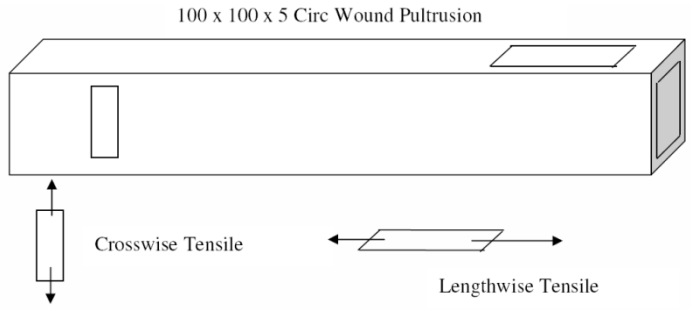

Figure 12 - Lengthwise & Crosswise

For the purpose of the tensile tests performed throughout this research project, only lengthwise direction were considered as this best represents the loading conditions in a composite bridge girder. The dimensions of the coupons comply with AS1145.4-2004, which are represented in the following figures.

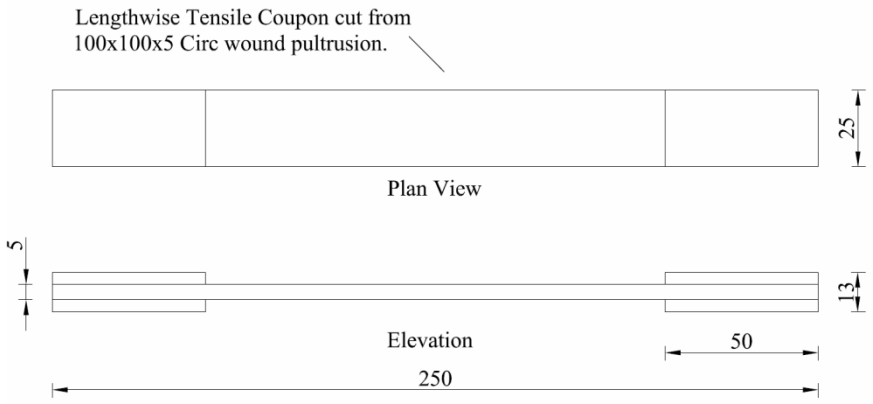

Figure 13 - Tensile Coupon Dimensions

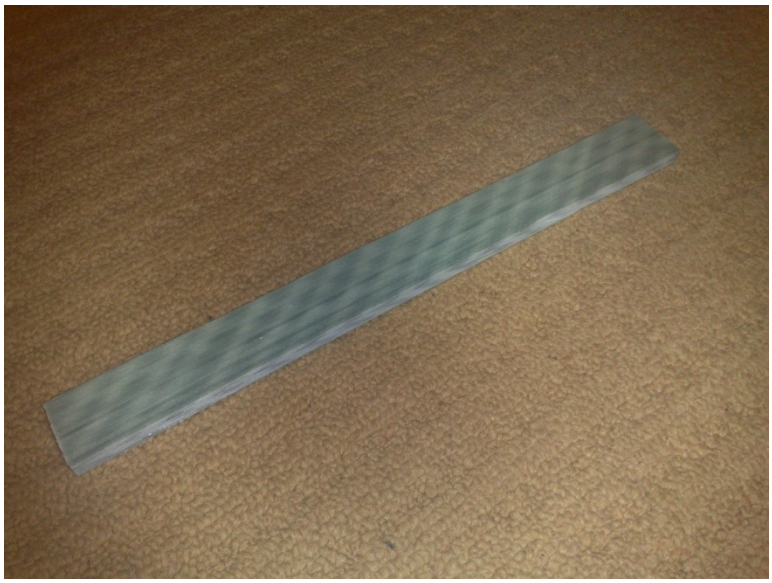

Figure 14 - FC Coupon without Tabs

Figure 15 - FC Coupons with Tabs

Table 1 below summarises the tests needed to be completed in order to determine the tensile properties. A minimum of five tests were completed to allow for any structural deviance within the samples. The expected theoretical maximum tensile loads are shown in Table 2 below.

Table 1 - Overview of Tensile Test Requirements

Test Orientation	No. of Specimens	Nominal Dimensions	Test Method	Properties Required and Notation
Lengthwise Tensile Coupons	5	25 mm wide by 250 mm long cut From one wall	ASTM D3036	σ_{ult} – Ultimate strength (MPa)

Table 2 - Theoretical Maximum Tensile Load

Coupon Name	Cross Sectional Area (mm^2)	Theoretical Maximum Tensile Load (N)
1	150	90,000
2	155	93,000
3	162	97,200
4	157	94,200
5	154	92,400
Mean =	155.6	93,360
Std Dev =	4.4	2,635.906
Char. Value =	148.4	**89,010.76**

3.2.3 Expected Results

Previous lengthwise tensile testing that has been undertaken on similar pultruded FC samples has shown an ultimate tensile stress, σ_{ult} (char. value) of 601.51 MPa, with a modulus, E equal to 32219.79 MPa. Results from testing are expected to be within 5% of this value as this is the known variability of structural characteristics. The value of ultimate tensile strength was calculated using the following equation:

$$Ultimate\ Strength\ (\sigma_{ult}) = \frac{max.\ force\ applied\ (F)}{cross\ sectional\ area\ (A)}$$

A stress versus elongation (or strain) was plotted so that a comparison of all testing results could be seen. This was done to see if there were and discrepancies in the results from testing. Upon completion of all tensile testing, the characteristic ultimate tensile strength (CUTS) was determined. The CUTS allows for any discrepancies in the composite material and is defined as the *Mean Value – 1.65 x Standard Deviations*. As said earlier the ultimate characteristic tensile strength forms the starting point for dynamic testing.

3.3 Dynamic Coupon Testing (Fatigue)

3.3.1 Overview

As stated in the previous section, the ultimate characteristic tensile strength forms the starting point of all dynamic (fatigue) coupon tests to come. Essentially for a given CUTS value, dynamic samples were tested at a percentage (85, 60, 50, etc) of this value. The CUTS value is equivalent to 100 percent ultimate stress and is considered to have one stress cycle. The purpose of fatigue testing was to determine

the fatigue behaviour (S-N curve) of pultruded FC. The figure below represents a typical composite fatigue curve.

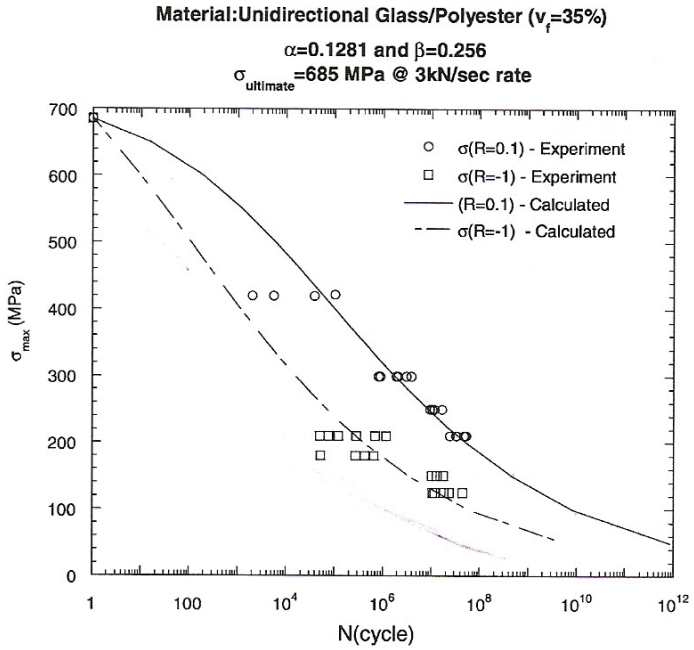

Source: Epaarachchi et al, 2003

Figure 16 - Typical Experimental S-N Curve

3.3.2 General Method

The fatigue coupons used were cut from the same FC samples as the tensile coupons. Dimensions of the coupons were also the same so that there was a consistency in results. As explained previously the test loads on the coupons were dependant directly on the results for the CUTS. For example, if the CUTS was equal to 601 MPa (results from previous tensile testing on similar samples), and the test percentage was equal to 90 percent, than the cyclic maximum stress inflicted on the coupon would be equal to 540.9 MPa. As described in Chapter 3 samples are subject to a stress ratio and load frequency. The testing methodologies used throughout this research project use a stress ratio of 0.1 (minimum/maximum stress) and load frequency of 5 Hz. A few experiments at lower frequencies have also been performed to show the affects frequency has on FC.

The testing procedure followed *ASTM D3479: Standard Test Method for Tension-Tension Fatigue of Polymer Matrix Composite Materials - Procedure A*.

> *Procedure A - A system in which the test control parameter is the load (stress) and the machine is controlled so that the test specimen is subjected to repetitive constant amplitude*

load cycles. In this procedure, the test control parameter may be described using either engineering stress or applied load as a constant amplitude fatigue variable.

The major results recorded are the number of cycles (N) and maximum/minimum stress each coupon has been placed under before it failed. If the coupon did not fail then a maximum of one million cycles was executed. This research project focused on high-stress and low-cycle cases so a maximum of one million cycles would theoretically never be reached. Ideally a minimum of five tests would produce more accurate results, however due to time constraints a minimum number of three tests were conducted at each stress percentage. The following table is a summary of the tests performed.

Table 3 – Overview of Fatigue Test Requirements

% of CUTS	No. of Specimens	Nominal Dimensions	Test Method	Properties Required and Notation
85	3	25 mm wide by 250 mm long cut From one wall	ASTM D3479	S – Fatigue Stress (MPa) N – No. Of Stress Cycles
60	3	25 mm wide by 250 mm long cut From one wall	ASTM D3479	S – Fatigue Stress (MPa) N – No. Of Stress Cycles
50	3	25 mm wide by 250 mm long cut From one wall	ASTM D3479	S – Fatigue Stress (MPa) N – No. Of Stress Cycles
40	3	25 mm wide by 250 mm long cut From one wall	ASTM D3479	S – Fatigue Stress (MPa) N – No. Of Stress Cycles

As shown in the table above, the experimental results do not explore the fatigue behaviour at low-stress, high-cycle cases. To determine the behaviour in the lower region a prediction model has been applied to the experimental data. The prediction model has been discussed in Chapter 5: Analysis & Discussions. The major object of fatigue testing is to determine the S-N curve which is represented in the following Chapter.

3.4 Composite Bridge Girder Testing

3.4.1 Overview

The purpose of testing the composite bridge girder was to further validate WCFT *"Bridging the Gap"* program. The fatigue test on the girder (cross section shown in

Figure 17) was one of many tests that had been completed in order to validate the design. The fatigue test would validate the girders long term fatigue performance and satisfy one of the many specifications set out by the Queensland Department of Main Roads (QMR).

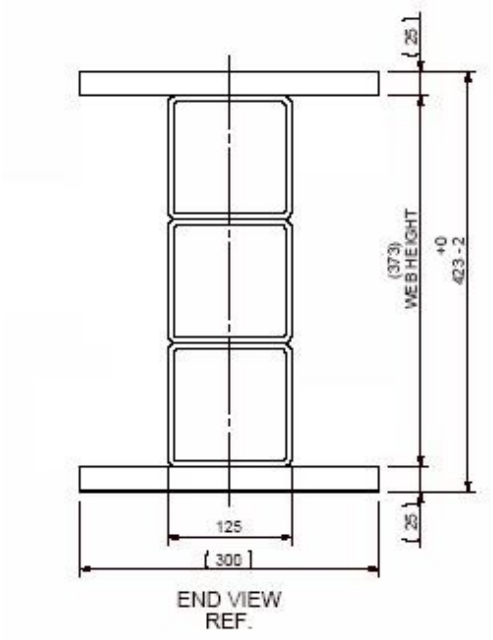

Figure 17 - Composite Girder Cross Section

QMR have strict guidelines which included a minimum of one million load cycles are tested at a serviceability live load of 109 kN.m. The fatigue test has been completed in two stages with the initial stage consisting of the one to 500,000 load cycles and the second stage the remainder of cycles to give a total of one million. The reason for this was purely because of time constraint issues. Stage 1 has been completed while stage 2 is still to be completed.

3.4.2 General Method

QMR specified that the fatigue test live load of 109 kN.m be used. Australian Standards (AS1170, Appendix B) suggests that this value be magnified by an appropriate factor to allow for the variability of structural units. WCFT has specified that the variability of structural units of pultrusion FC is 5%. This gives an appropriate factor of 1.20 which results in a test live load of 130.8 kN.m.

WCFT insisted that the performance of the composite girder be tested to its fullest limits. It was therefore decided that the test load be equivalent to the testing

machines maximum capacity of 240 kN.m (or 150 kN point load for the test setup), which is more than two times the requirement of QMR. A minimum test load was applied to the girder which was equal to 160 kN.m (100kN point load).

The test setup was under 4-point-bending as shown in Figure 18 and Figure 19 below. The reason for deciding 4-point-benidng was because it produces a constant moment between the loading points thus giving more accurate results. The maximum and minimum test loads (P) were equal to 150 kN and 100 kN respectively. The load was applied by a dynamic hydraulic actuator which followed a sinusoidal wave pattern at a cycle rate (frequency) of one hertz. Every 100,000 cycles a static point load of 200 kN was applied to girder. The purpose of this was to determine if there was and structural degradation within the beam throughout testing.

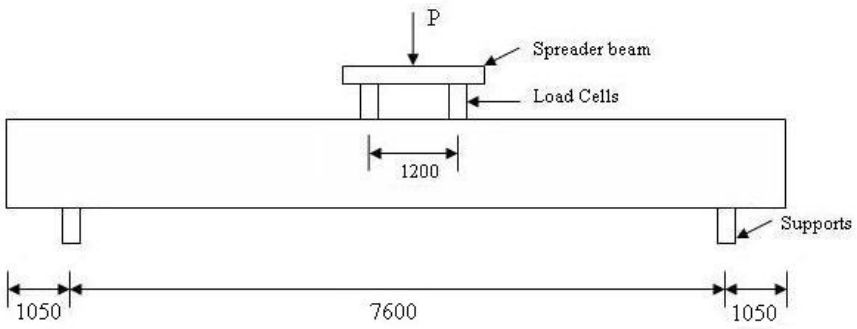

Figure 18 - Bending Fatigue Test Setup

Figure 19 - Bending Fatigue Test Setup

Results that were recorded for every static test included loads, defections and strains. The results would determine if there were and changes within in the girder such as loss in stiffness, creep, etc. The strain gauges were placed throughout the depth of the beam (Figure 20 below) so that the stress/ strain and neutral axis position could be determined.

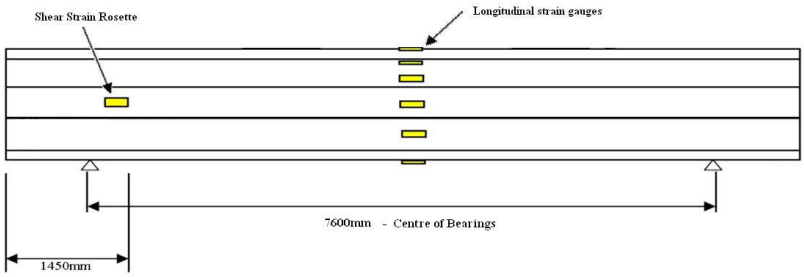

Figure 20 - Strain Gauge Locations

The composite girder has a theoretical bending stiffness of 2.8×10^{13} N.mm^2 which was given by WCFT. Testing will compare this value to the experimental results. The theoretical stresses at each of the strain gauge locations are given in Table 4 below. These results have been provided by WCFT.

Table 4 - Theoretical Stress

Stress Location	Theory Stress (MPa)
Top Flange	-75.3
Top Flange (underneath)	-66.7
Top Web	-37.9
Middle Web (neutral axis)	0
Bottom Web	37.9
Bottom Flange	75.3

NOTE: Negative stress indicates location is subject to compression

3.5 Summary

Chapter 3 summarised the methodologies used to determine the appropriate characteristic material properties of the pultruded fibre composites and the importance of each test. Such test procedures included tensile static and dynamic (fatigue) testing on coupons and large scale composite girder fatigue test. Results from coupon testing will determine whether or not small scale testing can be used as a means of predicting the fatigue life of large scale tests. These results have been discussed in the following chapters.

Chapter 4: Results & Discussions

4.1 Static Testing Results (Tensile)

As described in Chapter 3: Testing Methodology, before any dynamic testing could be undertaken the tensile properties of the pultruded fibre composite material must first be found. Tensile testing was done utilising the following setup in Figure 21 below.

Figure 21 - Coupon Undergoing Tensile Test

Each coupon was placed in the MTS (Material Testing System) Hydraulic Testing Machine grips under a constant a pressure. The first coupon tested was on the basis of a trial and error approach as the pressure required by the grips was unknown. The grip pressure had to be high enough so that there was no slippage between the grips and coupon, but also low enough so that the coupons would not fail as a result of too much pressure. Once the grip pressure was found, it was noted for the remaining tests to come. Each coupon was tested until failure. Previous research shows that the CUTS of the pultrusion FC has a theoretical value of 600 MPa.

It was expected that each coupon would reach a minimum load of 89 kN for satisfactory results. This was pushing the limits of the testing equipment as the machine was rated for a maximum load of 100 kN. The following table represents the results achieved for each of the coupons tested. As shown in Table 5 all but one

coupon achieved the minimum characteristic load of 89 kN. Table 6 is an example of the raw results that outputted from the MTS once all testing was completed

Table 5 - Summary of Tensile Testing Results

Coupon Name	Cross Sectional Area ($mm^{2)}$	Force (N)	Stress (MPa)
1	150	87,937.6	587.6
2	155	96,415.4	622.4
3	162	92,682.1	570.7
4	157	96,565.8	613.2
5	154	95,686.3	620.1
Mean =	155.6	93,857.44	602.8
Std Dev =	4.4	3,662.275	22.65535257
Char. Value =	148.4	87,814.69	565.4186683

Table 6 - Raw Results from MTS

Specime	Thickness	Width	Area	Peak	Peak	Break	Break
1	5.880	25.450	150	87938	587.64	86276	576.54
2	6.120	25.310	155	96415	622.45	****	****
3	6.460	25.140	162	92682	570.69	74563	459.12
4	6.180	25.480	157	96566	613.25	96292	611.51
5	6.140	25.130	154	95686	620.14	88853	575.85
Mean	**6.156**	**25.302**	**156**	**93857**	**602.83**	**86496**	**555.75**
Std Dev	**0.207**	**0.165**	**5**	**3662**	**22.68**	**9018**	**66.54**

The final results from tensile testing gave a CUTS value of 565.4 MPa. If the variability of structural elements (equal to 5%) is taken into consideration the results are considerably good. It should be noted that the samples used for all testing are not perfect samples as they have sustained minor defects during the pultrusion process. Gathering all the results from tensile testing together, Figure 22 is produced, which is a plot of the tensile load versus the elongation of the coupons tested, which is similar to a stress-strain plot.

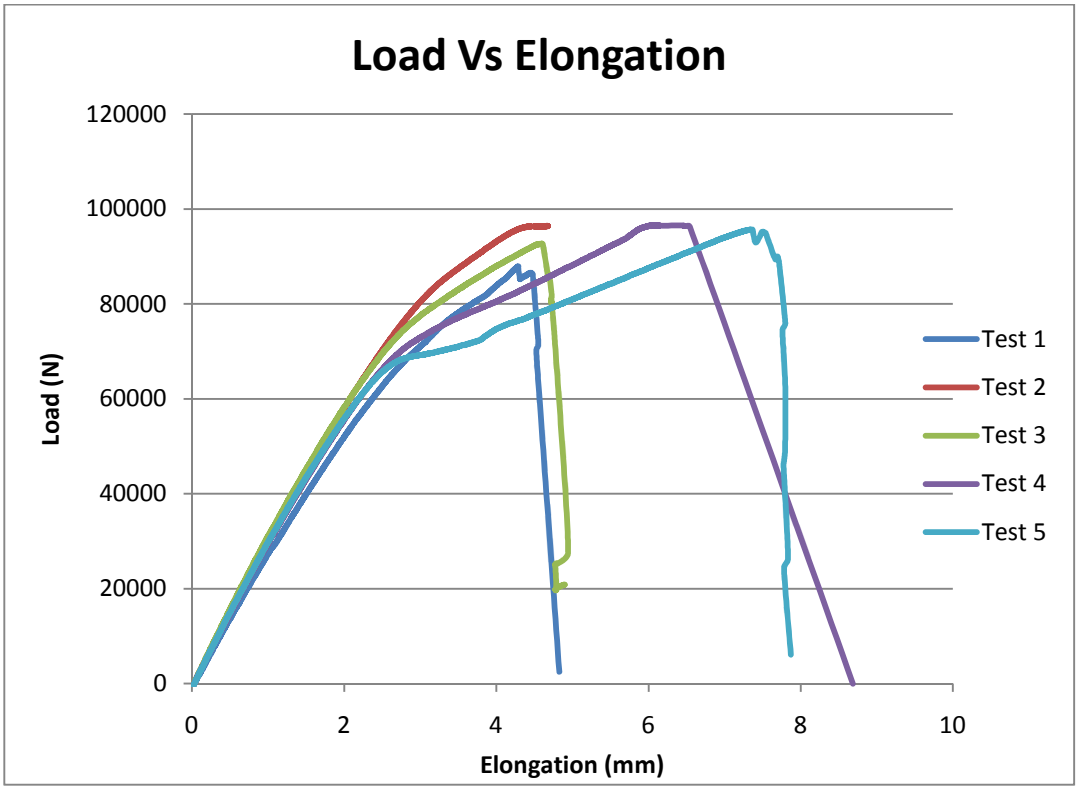

Figure 22 - Load vs. Elongation for Pultrusion

From Figure 22 above it can be seen that *tests 4* and *5* reached a much higher elongation than the remaining tests. This is because of slippage between the grips and coupons. When a slippage was noticed in the results that were displayed on screen, the pressure in the grips was increased so that this would no longer occur. It can be seen that these two coupons still reach an ultimate tensile load similar to that of the remaining tests. These results show to be very consistent, thus being considered to be reliable. Being a very brittle material, there was no warning within the coupon before it failed as shown in Figure 23 which represents the failure modes of the five coupons tested.

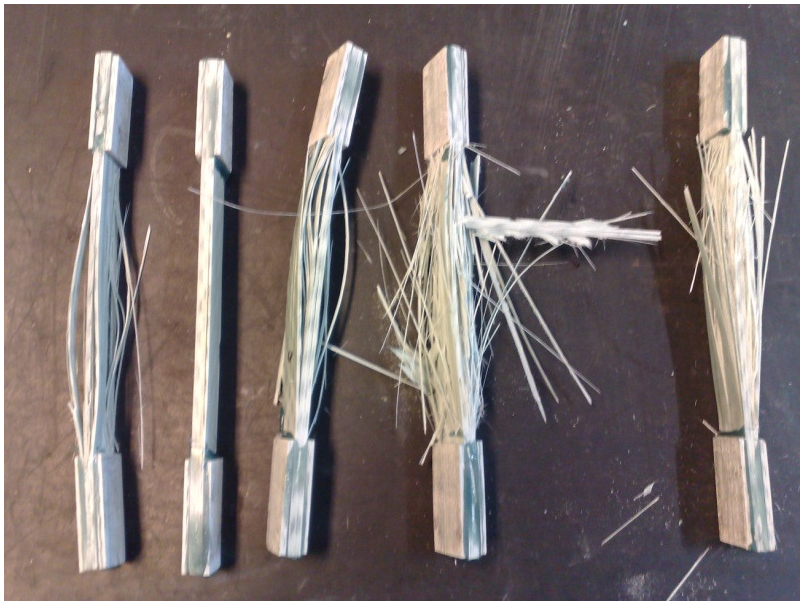

Figure 23 - Pultrusion Coupon Failures

The pultrusion FC failure is unlike a metal alloy tensile failure where a necking phenomenon occurs (Figure 24) between the grips before it fails. This was expected as the makeup of FC material is considerably different to a metallic material. It was difficult to determine when the coupons were going to fail. It was noted during the test, that the speed in which the coupon began to elongate or stretch, began to rise rapidly towards the end of the test leading to ultimate failure. As shown in the figure above, the coupons shattered upon failure rather than having a clean break through the middle. As explained in Chapter 2: Literature Review the composite material is made up of a glass fibres and resins which results in a brittle material. FC behaves much like glass when it shatters.

(Source: upload.wikimedia.org/.../6f/Al_tensile_test.jpg)

Figure 24 – Metal Alloy Necking

The results from the static tensile testing proved to be reliable as all five test coupons appeared to have failed in a similar matter and ultimate stress. The standard deviation for tensile stress of the pultrusion is very low at 22 MPa which shows there is a good consistency within the material. The characteristic ultimate tensile stress (Su = 565.42 MPa) of the samples tested was however, found to be lower than previous testing (600 MPa). This was not a major worry as this is close to a five percent error and considering the history behind the manufacturing process, is rather good.

4.2 Dynamic Testing Results (Fatigue)

As stated in Chapter 3: Testing Methodology a minimum of three tests was undertaken at each individual stress value. The stress values that were tested were determined primarily on the basis of test duration. As it was initially expected that testing at low-stress/ high-cycle situations would take a great deal of time to complete, the tests were focused on high-stress/ low-cycle situations. However the results will show that low-stress/ high-cycle situations did not take as long to complete as originally expected.

Each sample was tested at a frequency of five Hertz (five cycles per second). This value was chosen to increase the speed of the tests. It will be discussed later on in this chapter the effects frequency has on a FC sample. As stated in Chapter 3 the dynamic testing has been focused on tension-tension testing mechanism, which results in the coupons not being placed under a compressive load.

To ensure the coupons were not placed under a compressive load a maximum and minimum stress was applied during the test. The ratio of minimum stress to maximum stress is known as the *stress ratio*. For the testing undertaken on the pultruded FC coupons, the value of R was equal to 0.1, which means the minimum stress during testing was equivalent to 10% of the maximum stress. Figure 25 below shows that each specimen is subject to a tension force only as a minimum and maximum axial force has been recorded. The example is for a coupon that was tested at 40% of CUTS value. If a compression force was recorded then this would show as a negative value on the figure. All axial loads are positive and above the x-axis.

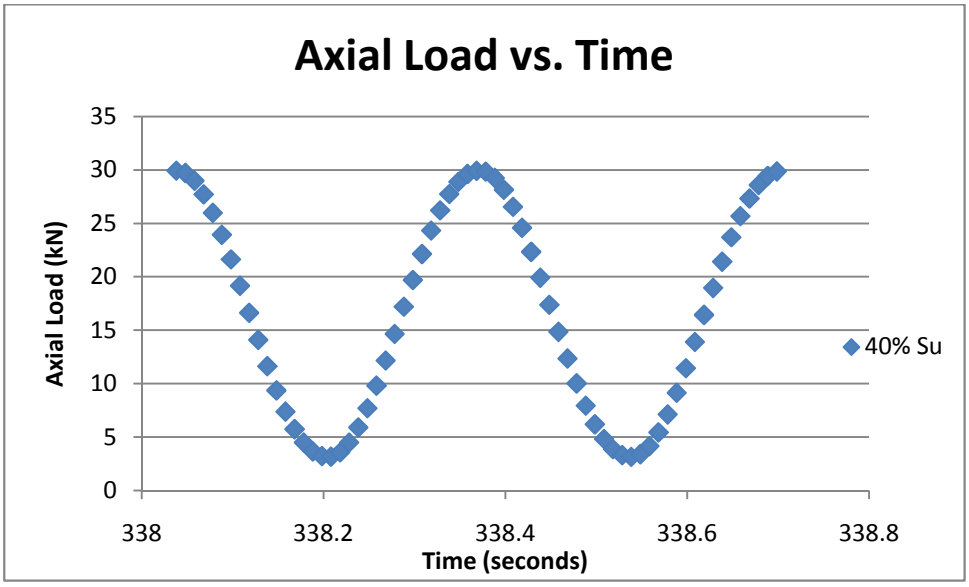

Figure 25 - Example of Stress Ration

No strains were recorded as the ultimate goal was to record the number of cycles a specimen sustained upon failure. An example of the final destruction of a fatigue tested coupon is shown in Figure 26.

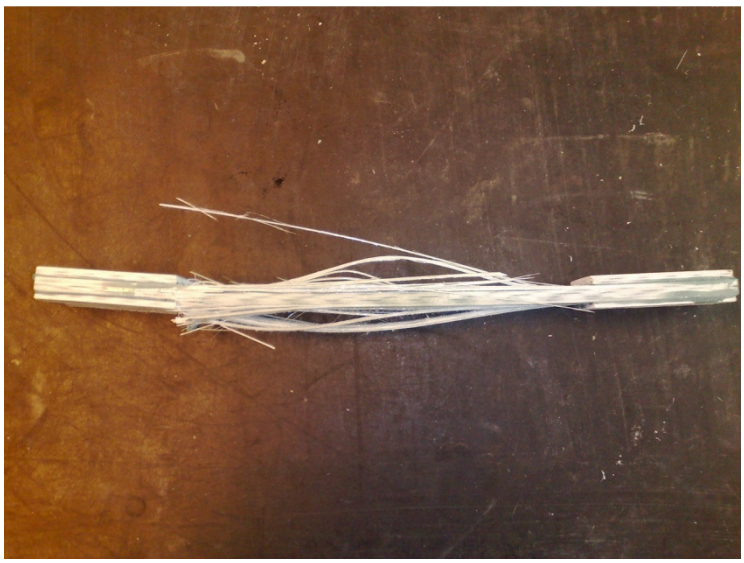

Figure 26 - Typical Fatigue Failure

Once all the tests were complete they were tabulated as shown in Table 7. As expected, when the stress imposed on the coupons decreased the number of cycles achieved by each coupon increased. This has been discussed in theory in Chapter 2. As noted earlier it was expected that for a low-stress/ high-cycle (40 percent of ultimate stress for example) case, the coupons would be achieving very high cycle ranges such as around the one million mark. However it can be seen in the results

that for coupons tested at 40 percent of ultimate stress, the maximum number of cycles reached was only equal to 20,830 cycles. This is rather low especially when compared to metal fatigue.

Table 7 - Summary of Dynamic Testing Results

Coupon Name	Width (mm)	Thickness (mm)	Area (mm^2)	Load (N)	Max. Stress (MPa)	Min. Stress (MPa)	% of Su	N (cycles)
85%-1	25.07	5.34	133.8738	65000	485.5319	48.55319	85.871	450
85%-2	25.14	5.47	137.5158	65000	472.673	47.2673	83.5968	360
85%-3	25.75	5.38	138.535	65000	469.1955	46.91955	82.9818	280
60%-1	25.167	5.25	132.12675	45000	340.5821	34.05821	60.2352	1600
60%-2	25.57	5.267	134.67719	45000	334.1323	33.41323	59.0945	1000
60%-3	25.05	5.34	133.767	45000	336.4058	33.64058	59.4966	1400
60%-4	25.23	5.28	133.2144	45000	337.8013	33.78013	59.7434	800
50%-1	25.19	5.08	127.9652	37500	293.0484	29.30484	51.8285	4542
50%-2	25.27	4.99	126.0973	37500	297.3894	29.73894	52.5962	1625
50%-3	24.13	5	120.65	37500	310.8164	31.08164	54.9709	4234
40%-1	26.02	5.04	131.1408	30000	228.7618	22.87618	40.4587	10000
40%-2	25.23	4.96	125.1408	30000	239.73	23.973	42.3986	20830
40%-3	25.05	5.1	127.755	30000	234.8245	23.48245	41.531	17315

Theory suggests (Chapter 2: Literature Review) that the stress value a metal alloy achieved at 5 million cycles [Australian Standards, AS4100] is considered to be the endurance limit or the limit where the material will withstand an infinite number of cycles. This is usually around the 50 percent of ultimate stress range and is true for most metal alloys. The results from dynamic coupon testing show that for a specimen tested at 50 percent of ultimate stress, it was only reaching an average number of 4,388 cycles (not including the outlier). This was considered to be rather low and final discussions will be made in Chapter 6: Conclusions.

After tabulating the results, an S-N curve (or fatigue curve) can be plotted for the pultruded fibre composites. As stated previously the S-N curve represents the maximum stress (S) the material sustains versus the number of cycles (N) achieved. Figure 27 represents the S-N curve achieved from testing of the pultruded fibre composite samples.

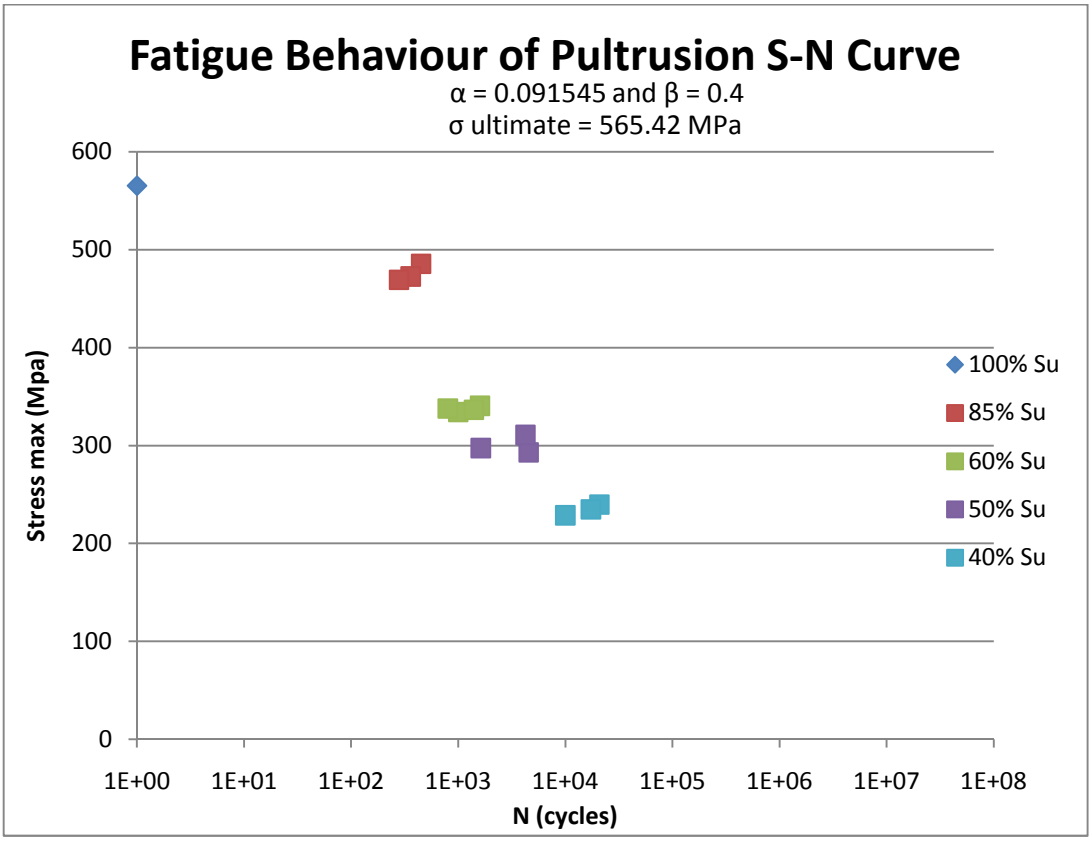

Figure 27 - Experimental S-N Curve for Pultrusion

Figure 27 shows that for each stress value tested the results were consistent. It also shows that for a decrease in stress there was an increase in cycles, which was expected.

It should be noted that the tests were load controlled, meaning that a consistent load was placed on each of the coupons at the different stress values (as shown in the table above). In reality this gives a different percentage of ultimate stress because each coupon cross sectional area varies slightly. For example, for coupons tested at a maximum load of 65 kN, the percentage of ultimate stress for each coupon was 85.87, 83.59 and 82.98 respectively, which is near enough to the 85 percent that needed to be achieved. It was believed that during testing, keeping the load constant would mean a comparison could be made between the minor stress differences and cycles for each data set. Figure 28 below represents the results for all tests at 85% of ultimate characteristic stress. Theoretically as the stress on the samples is increased, the number of cycles is decreased, however as it can be seen in the figure below this is not the case. What this proves is there is variability within the manufacturing of the material.

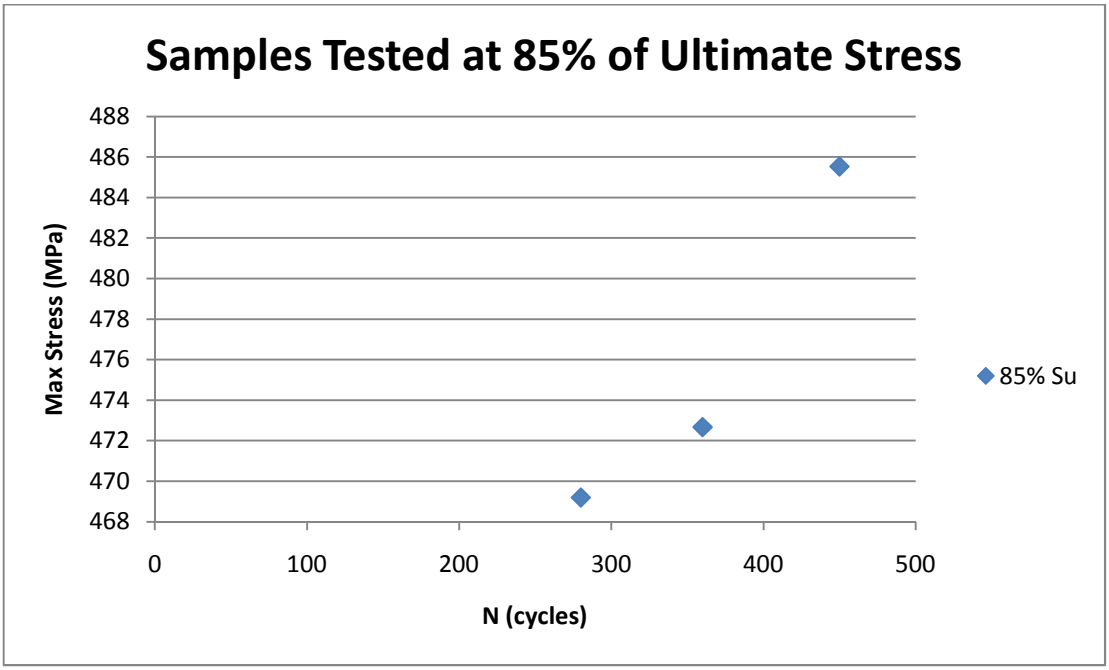

Figure 28 – Plot Showing the Difference in Maximum Stresses

As explained earlier the effects of the frequency at which the dynamic test is undertaken is very minimal on the coupons. In fact it was found by decreasing the frequency; the coupons sustained a reduced number of cycles as shown in Table 8.

Table 8 - Results of Coupons at Different Frequencies

Coupon Name	Width (mm)	Thickness (mm)	Area (mm^2)	Load (N)	Stress (MPa)	% of Su	N (cycles)
85%-1 (1Hz)	25.74	5.157	132.74118	65000	489.6747	0.866037	277
85%-2 (1Hz)	25.13	4.96	124.6448	65000	521.4818	0.922291	269
60%-1 (1Hz)	25.34	5.14	130.2476	45000	345.4958	0.611043	899

However, this does not say that if the frequency was to be continually increased, the fatigue life would continually be extended. The effects of increased frequency and increased fatigue life are based primarily on the absence of temperature. If a temperature rise was evident then a decrease in the fatigue life would also occur due to the decrease in structural properties. This dissertation does not look at the effects of temperature on a pultruded fibre composite fatigue life.

4.3 Composite Beam Fatigue Results

Fatigue testing the composite bridge girder had two purposes. The first purpose was to satisfy the requirements of Queensland Main Roads and the second to compare

those results to coupon testing results which have been outlined in the previous section. Figure 29 below shows the girder undergoing fatigue testing. As the girder wasn't actually tested to destruction like the coupons were, it makes it a little hard to actually compare results. The prediction model (discussed in Chapter 5) will be used to help clarify these results and make a comparison between bridge girder and coupons.

Figure 29 - Composite Girder Undergoing Fatigue Testing

Figure 30 and Figure 31 below shows the strain data for the initial and 100,000 cycle's static test respectively. It can be seen that all the strains measured (and therefore stresses) remains constant throughout the duration of the testing, indicating that no damage and loss in stiffness had occurred within the girder. Essentially no strains were recorded at the centre of the web indicating that the position of the neutral axis did not change throughout the testing. As both figures are almost identical, there is no loss of structural prosperities over the first 100,000 cycles.

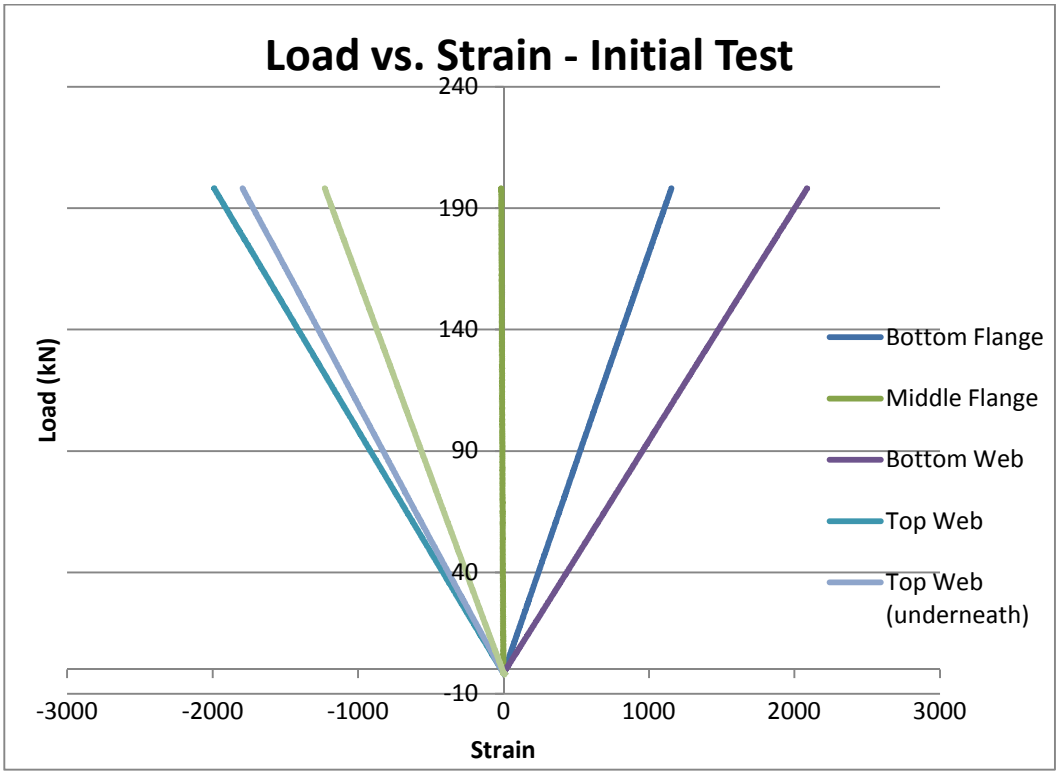

Figure 30 - Load vs. Strain data Initial Test

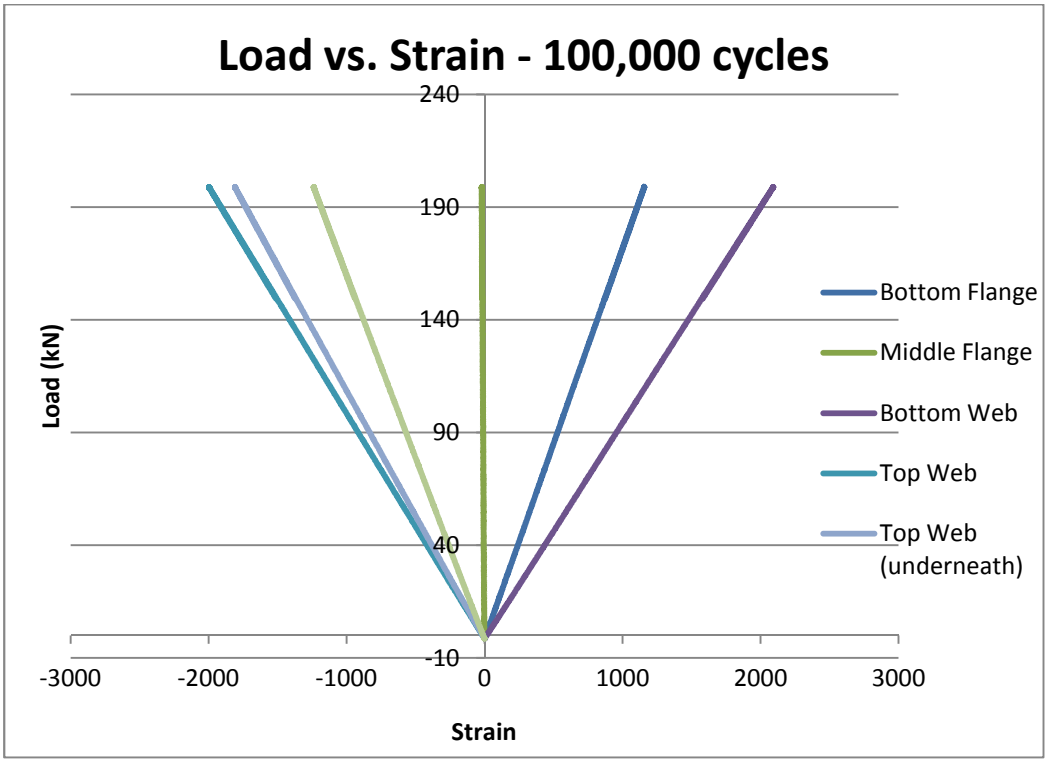

Figure 31 - Load vs. Strain data 100,000 cycles

Without shown countless figures of what is shown above, the structural fatigue performance of the girder can be shown through the deflection. If the girder was

subject to greater deflection after 500,000 cycles it would be assumed that there was a loss in bending stiffness. Figure 32 below represents the load versus the deflection for the five static tests. It can be seen that the load deflection curve is linear throughout the test and does not deviate from its initial path. There is a slight increase in stiffness between the initial and final test, however this difference is minimal and can be attributed to errors in measurement and compression of the rubber mats placed at the load points and supports. There are no sharp spikes in the figure indicating there are no structural failures occurring during the testing. The reason why the deflection is negative is because the strong pull reduces in length when a load is applied.

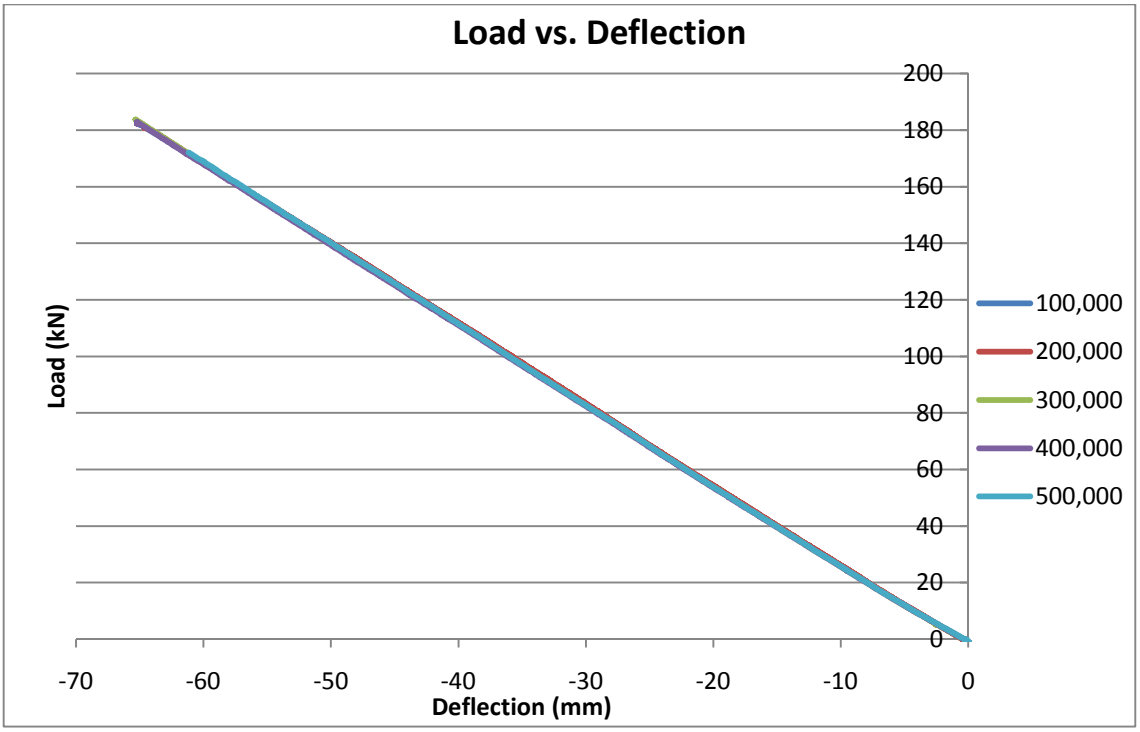

Figure 32 - Load vs. Deflection for every 100,000 cycles

The bending stiffness was calculated using the following formula which relates to Figure 33. The purpose of determining the bending stiffness is to see whether the girder is subject to structural failure as a result of fatigue damage. The results from testing show that there is no deviance in the bending stiffness (Table 9).

$$EI = \frac{Pa}{24\Delta}(3L^2 - 4a^2)$$

Where:

$\Delta = deflection\ at\ centre$

$P = Maximum\ test\ load$

$a = distance\ from\ load\ point\ to\ support$

$L = distance\ between\ supports$

$EI = bending\ stiffness$

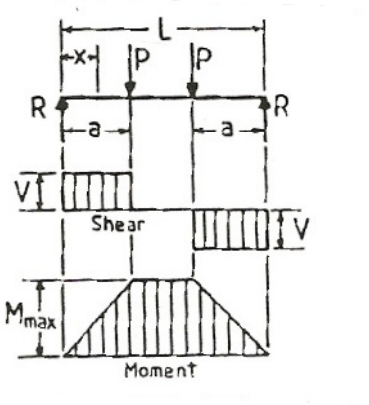

Figure 33 - Deflection Calculation

As explained in Chapter 3, a static test was applied to the beam every 100,000 cycles. The experimental bending stiffness (EI) recorded from each of these tests is shown in Table 9. The results from static tests show a mean difference of 3.43% compared to the theoretical values given by WCFT. These are considered to be good results as there are some variability's within testing producing including the compression of the rubber mats under the supports which would yield slightly different results.

Table 9 - Experimental EI vs. Theoretical EI

Cycles	Experimental *EI*	Theory *EI*	Difference %
100,000	2.70114E+13	2.80E+13	3.53%
200,000	2.70344E+13	2.80E+13	3.45%
300,000	2.70852E+13	2.80E+13	3.27%
400,000	2.69836E+13	2.80E+13	3.63%
500,000	2.70867E+13	2.80E+13	3.26%
Mean =	**2.70403E+13**	**2.8E+13**	**3.43%**

As stated in Chapter 3, the theoretical stresses at each of the strain gauge locations were given by WCFT with the experimental results shown in Table 10 below. The neutral axis shows a slight stress which is probably due to inaccuracies in the test

setup, such as strain gauge location, distance between supports, etc. The stresses from the experimental data were found using the following equation:

$$\sigma = E \times \varepsilon$$

Where:

$\sigma = normal\ stress$

$E = Tensile\ Modulus$

$\varepsilon = measured\ strain$

Table 10 - Experimental vs. Theory Normal Stress

Stress Location	Experimental Stress (MPa)	Theory Stress (MPa)	Difference %
Top Flange	-78.50	-75.3	-4.25%
Top Flange (underneath)	-71.09	-66.7	-6.59%
Top Web	-41.37	-37.9	-9.16%
Middle Web (neutral axis)	-0.56	0	
Bottom Web	38.75	37.9	-2.24%
Bottom Flange	82.19	75.3	-9.15%
Mean =			**-6.28%**

4.4 Summary

As stated before the composite bridge girder wasn't actually tested to destruction. This therefore makes it hard to compare its results to coupon testing. To actually test the girder to fit the S-N curve generated by coupon testing would mean a minimum number of around 278 million cycles would need to be tested. Testing at one hertz continuously means this would take around nine years (500,000 cycles took 11 days to complete with interruptions). This would cost a lot of time and money to actually do the test and would be impracticable. The prediction model as described in the following chapter will help determine how many cycles the girder will be able to sustain before failure under its current loading conditions. The results from coupon testing showed a typical behaviour of fatigue testing as the number of cycles increased when the stress was reduced. This is typical of all fatigue tests. The tensile testing shown good results with all samples breaking at a similar load and manner.

Chapter 5: Analysis & Discussions

5.1 S-N Curve Prediction Model

5.1.1 The Model

In most instances it is impracticable to test specimens in a low-stress/ high-cycle situation as these tests can take a great deal of time to complete. This is where the prediction model is useful as it can predict the fatigue behaviour of a material using a well-defined minimum number of tests (Epaarachchi et al, 2003). The prediction model used as part of this research project was developed by Epaarachchi and Clausen.

Both Epaarachchi and Clausen developed the model as they believed current models did 'not accurately consider the effects of load stress ratios and load frequencies'. They used fatigue data from literature and selected research laboratories were used to test the models accuracy. They found the model 'to be in good agreement with all experimental data' proving that the model will be an accurate choice to predict the fatigue behaviour of pultruded fibre composites.

There is a lot of theory behind the prediction model; however since this is not the focus of this research project, only the important methods have been discussed. The determination of the prediction model involves three major steps. The first of these steps is to perform the initial dynamic (fatigue) tests. The second step is to determine the material constants alpha and beta and the third step is to apply the prediction model equations to determine the fatigue curve.

5.1.2 Material Constants

Alpha (α) and Beta (β) are material constants that were determined from the experimental data. For a given data set (for example the three tests that were carried out at 85 percent of ultimate stress) alpha and beta were determined on a trial and error basis by using the following equation.

$$D = \alpha(N^{\beta} - 1) = \left(\frac{\sigma_u}{\sigma_{max}} - 1\right)\left(\frac{\sigma_u}{\sigma_{max}}\right)^{0.6-\psi^*|sin\theta|} \frac{1}{(1-\psi')^{1.6-\psi^*|sin\theta|}} f^{\beta}$$

Where:

$\sigma_u = Ultimate\ Stres$

$\sigma_{max} = Maximum\ stress\ in\ a\ sample$

$\psi^*, \psi^{'} = material\ constants$

$N = Number\ of\ cycles$

$\theta = smallest\ angle\ between\ the\ fibre\ direction\ in\ loading$

$f = Frequency$

By using the results as found in Chapter 4: Results & Discussions and by assuming a trial value of beta, *'D'* and *'N^{β}-1'* was determined for each given data set. By plotting *'D'* against *'N^{β}-1'* Figure 34was calculated.

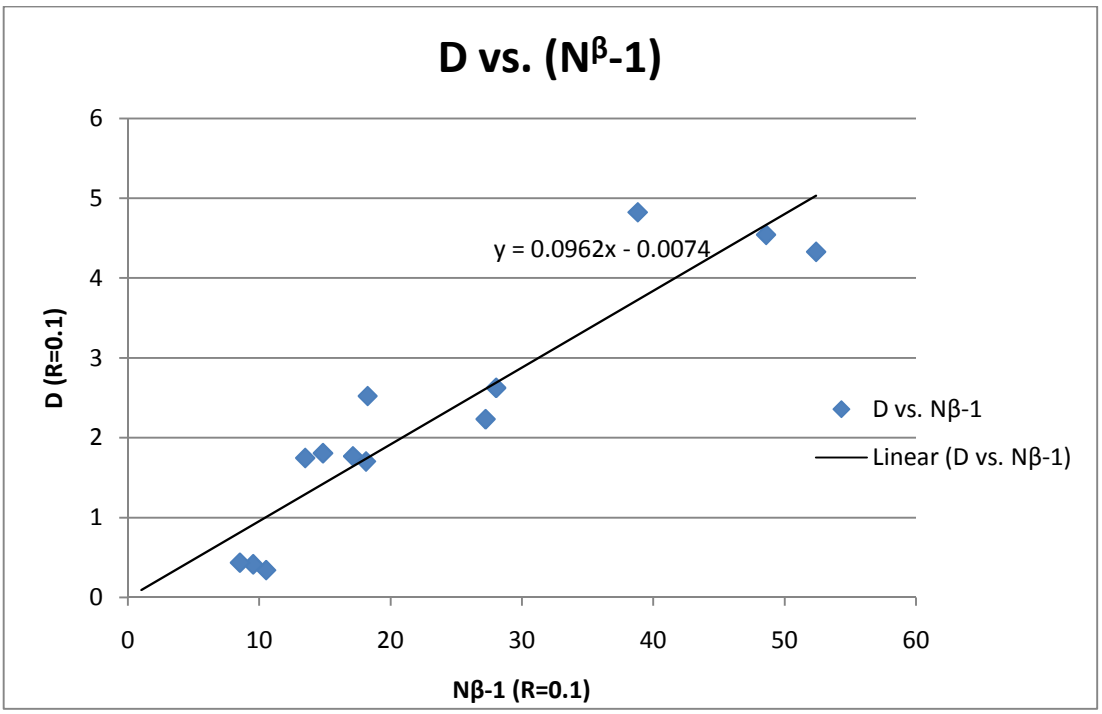

Figure 34 - Material Constants Alpha & Beta

The goal of the trial and error process is to construct a linear regression line (shown in the above figure) that passes through origin. In simple terms the trial value of beta will be continually changing until the linear regression equation is equal to y = m(x) + 0. Once the final value of beta was found, alpha was determined for each data set using the following equation.

$$D/\alpha = (N^{\beta} - 1)$$

Once the individual values of alpha were determined for each experimental data set, the mean value alpha was noted. Table 11 below represents the results of alpha and beta.

Table 11 - Determining Alpha & Beta

Description	Alpha (α)	Beta (β)	D	(N^{β}-1)
85%-1	0.032637136	0.4	0.343197715	10.51556
85%-2	0.043633325	0.4	0.415923593	9.532246
85%-3	0.051219785	0.4	0.43664668	8.524961
60%-1	0.093971976	0.4	1.703434705	18.12705
60%-2	0.12167419	0.4	1.806731767	14.84893
60%-3	0.103294573	0.4	1.769666357	17.13223
60%-4	0.1294698	0.4	1.747271766	13.49559
50%-1	0.093625188	0.4	2.624638329	28.03346
50%-2	0.138262923	0.4	2.522750592	18.24604
50%-3	0.082003464	0.4	2.232898162	27.22932
40%-1	0.12423238	0.4	4.821547733	38.81072
40%-2	0.082602836	0.4	4.327722883	52.39194
40%-3	0.093453818	0.4	4.540653092	48.58713
Mean =	**0.091545**			

5.1.3 Applying the Model

The final step of the model was to determine the theoretical maximum stresses and cycles for the given material constants. Once again the following equations were used.

$$D = \left(\frac{\sigma_u}{\sigma_{max}} - 1\right)\left(\frac{\sigma_u}{\sigma_{max}}\right)^{0.6-\psi^*|sin\theta|} \frac{1}{(1-\psi')^{1.6-\psi^*|sin\theta|}} f^{\beta}$$

&

$$D/\alpha = (N^{\beta} - 1)$$

The stress is found from the percentage of ultimate stress. For example, 80 percent of 565.42 MPa is equal to 452.34 MPa. The number of cycles for each percentage of ultimate stress is found first by calculating *'D'* from the first equation above and then rearranging the second equation so that it is equal to the number of cycles. The results in 5 percent intervals are represented in Table 12 below.

Table 12 - Prediction Model Results

% of Su	σ_{max}	D	N (cycles)
100%	565.42	0	1.00E+00
95%	537.149	0.103323768	6.61E+00
90%	508.878	0.225320127	2.23E+01
85%	480.607	0.370347127	5.72E+01
80%	452.336	0.544094102	1.27E+02
75%	424.065	0.75410182	2.59E+02
70%	395.794	1.010537402	5.03E+02
65%	367.523	1.327378184	9.46E+02
60%	339.252	1.72427286	1.75E+03
55%	310.981	2.229565381	3.24E+03
50%	282.71	2.885399812	6.03E+03
45%	254.439	3.756735936	1.15E+04
40%	226.168	4.948154665	2.25E+04
35%	197.897	6.637315888	4.63E+04
30%	169.626	9.147281286	1.02E+05
25%	141.355	13.12034489	2.50E+05
20%	113.084	20	7.14E+05
15%	84.813	33.67137976	2.61E+06
10%	56.542	68.20724549	1.52E+07
5%	28.271	218.2526874	2.78E+08

The results from the table above can then be plotted onto the same S-N curve as determined in Chapter 4: Results & Discussions. As seen in the experimental results the lower the maximum stress inflicted on the material the higher the number of cycles achieved. Figure 35 below represents these results and shows a comparison between experimental and prediction model results.

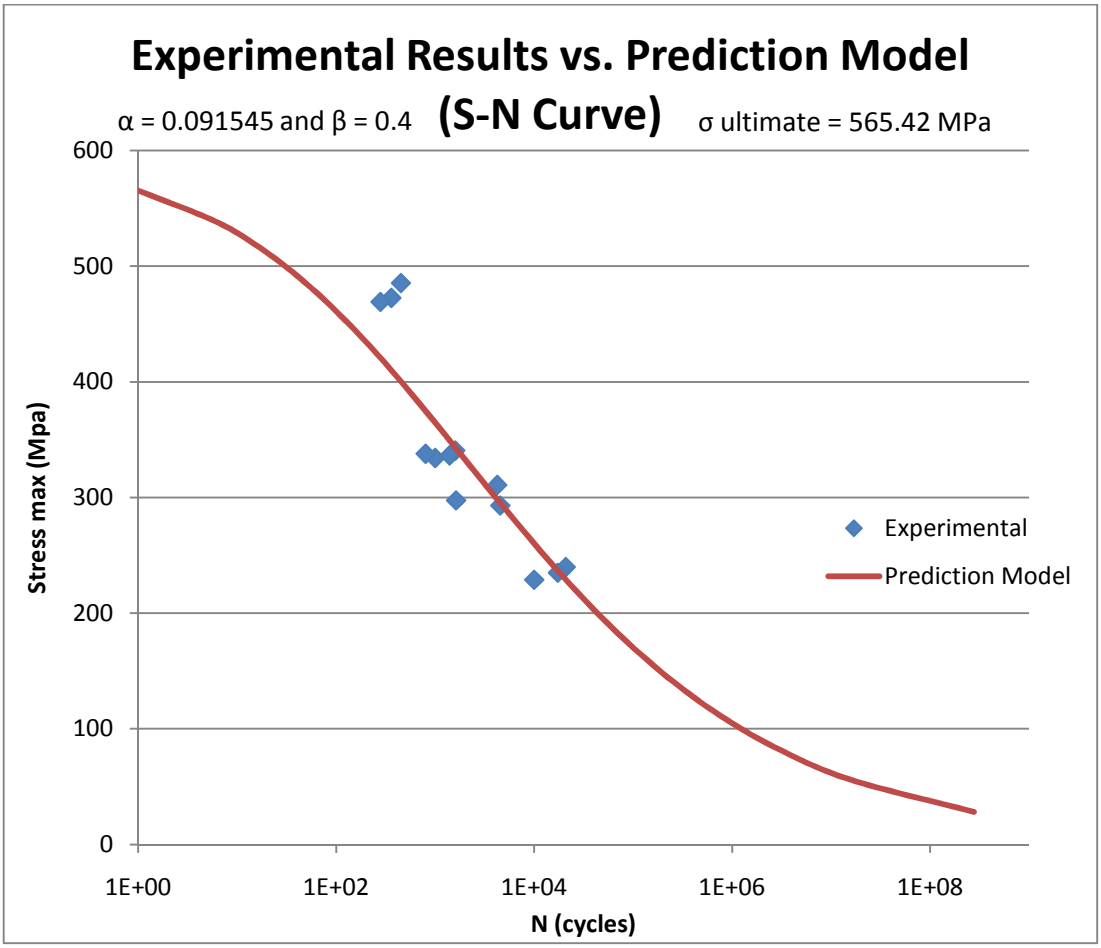

Figure 35 - Experimental versus Prediction Model

As shown in Figure 35, the prediction model gives a good indication on the fatigue performance of the pultruded composite in the low-stress/ high-cycle end of the curve. It can also been seen that the model fits the experimental data rather well thus proving to be an accurate model. The only outliers from the experimental results are those that were tested at 85 percent of ultimate stress. Reasons for this aren't known but the most probable cause is because the ultimate characteristic stress used in calculations is a lesser value than the mean calculated stress. It other words if the mean value was used in the calculations instead of the characteristic stress the maximum stress for the prediction model would be a higher. The accuracy of the model still needs to be proven though, as more testing in the low-stress/ high-cycle situations would need to be done to determine how accurate the model really is.

5.2 Small Scale versus Large Scale Testing

As stated earlier the composite bridge girder fatigue test doesn't actually represent the coupon results as it wasn't tested to destruction. However the fatigue life of the

girder can be predicted using the prediction model described in the previous section. Firstly it must be noted that the composite girder is made from two different types of pultrusion material. The flanges are sourced from an external company where as the web is manufactured by WCFT and is the main focus of this research project. A reminder should also be made that the composite girder has been tested at twice the serviceability load specified by QMR.

Theory states that the maximum stress within WCFT pultrusion will be the point furthest away from the neutral axis. Strains were not recorded at this point throughout testing. The closest strain recorded in the experiment was in the middle of the bottom or top web, which recorded stresses of 38.75 MPa 41.37 MPa respectively. As coupon testing was conducted on a tension-tension basis, only the stress under tension will be considered for discussion. The theoretical stress calculated in the bottom web is equal to 37.9 MPa which gives an error of 2.24%. Figure 36 below shows the area where a typical girder is expected to perform in terms of fatigue.

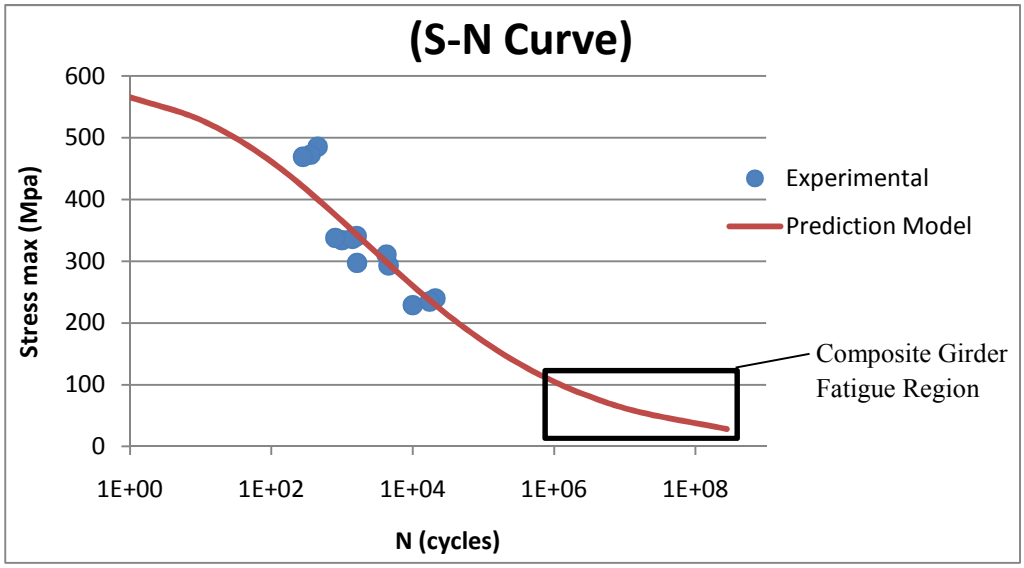

Figure 36 - Location of Girder Fatigue on S-N Curve

According to the prediction model theories, a maximum number 75 million cycles would be reached at a stress of 38.75 MPa. If a test was to be conducted at this magnitude, the duration of the test would take approximately 868 days (almost two and a half years) to complete. Even at a maximum stress of 82.19 MPa (highest recorded in the girder) would take approximately 35 days to complete (three million

cycles). In the low regions of the S-N curve, slight differences in stresses can mean a large difference in the maximum number of cycles.

5.3 Summary

This chapter gave an insight into using a prediction model for the given experimental data. It explored the limitations of model and the methods used to determine the final S-N curve. There is more theory involved in the determination of model but as stated earlier this is not the focus of this research project. More detail of the model can be found in Epaarachchi and Clausen paper titled *'An empirical model for fatigue behaviour prediction of glass fibre-reinforced plastic composites for various stress ratios and test frequencies'*.

The chapter also discussed the relevance of small scale and large scale testing and made a comparison between the two. To test a coupon at similar stress levels achieved in girder would mean testing it to roughly 75 million cycles. If the test was undertaken at the same frequency as previous coupon testing (five hertz) this would mean the test would run for approximately 173 days which is considered to be impracticable. Like wise to achieve the same stress states in the girder as the coupons did (minimum of 240 MPa), would mean a moment load of 1521 kN.m would need to be applied. For the test setup used this is equivalent to a point load of 475 kN which goes beyond the limits of the testing equipment.

Chapter 6: Conclusions & Recommendations

This chapter provides a summary of the results and recommendations that have been presented throughout this dissertation. The chapter will summarise the results and work involved throughout the research project and recommendations for future work in this field of study.

6.1 Key Findings

This research project aimed to complete two major objectives. The first of these objects was to investigate the fatigue behaviour of pultruded fibre composites, and the second objective was to perform small scale tests to extrapolate the same results as for large scale girders.

The investigation into the fatigue behaviour of FC has shown that they do not exhibit the same behaviour as other conventional materials such as steel and concrete. Standards around the world show that a metal alloys have an endurance limit which is the stress limit that is considered to have an infinite number of stress cycles. The literature researched throughout this project has shown that FC does not have this property. However no such experimental data could be found to confirm this theory.

6.1.1 Dynamic Coupons

The small scale testing was undertaken on pultruded FC coupons which were sourced from the same batch of material. It has been found from testing that the FC samples exhibit strong tensile properties, but poor fatigue properties. Tensile testing showed consistence results with all samples breaking at a similar stress and manner. Tensile samples tended to shatter upon failure. This was due to the glass like behaviour of the material. The failure mode also demonstrated that samples were likely to break in the direction of the load being applied. This was because the 0^{o} fibres were taking all the force when placed under a tensile load. So they were most likely to break first.

The fatigue samples failure mode was rather different to the tensile samples with the majority of the samples breaking close the testing equipments grips. It was first originally thought that there was too much pressure being applied to the fatigue samples. However even after the pressure had been reduced the samples still failed in

a similar manner. This type of failure was most likely the cause of the poor results obtained from fatigue testing.

The cyclic testing at the highest stress (85% of ultimate stress) showed particularly good results, when compared to existing fatigue studies; however the results seemed to be considerably poor from there on. The high stress within the grips is the most likely cause contributed to the samples breaking a lot early than expected. Placing chamfers on the tabs would help reduce this problem; however testing guidelines did not recommend this. Further research into the use of chamfered tabs and the stress distribution within the tabs should be considered for further experiments. As fatigue testing is a lengthy process, and there was insufficient time to research this.

6.1.2 Composite Bridge Girder

Unlike the fatigue coupon samples, the composite bridge girder produced good results from the initial 500,000 cycles tested. Considering the girder was subject to a serviceability load more than double what was expected by Queensland Main Roads the girder showed no signs of structural failure. No creep effects were evident, as stresses and deflections remained constant over each of the static tests conducted at 100,000 cycle intervals. This was expected as the internal stresses in the individual components are quite low. It should be noted that due to a mechanical error in the testing equipment a further 500,000 cycles was not able to be completed when this dissertation was submitted.

It was hard to compare the results from the large scale tests to the small scale tests as they were both tested in different stress ranges. It would have been a lengthy process to test coupons at the stress levels the girder was subject to and on the other hand the testing equipment was not able to test the girder to the high stress levels the coupons were subject too. The prediction model however breaches the gap between the two, and gives an insight into what the fatigue life of the girder. The model shows that the girder can withstand up to 75 million cycles when subject to test conditions. If the working live moment specified by QMR was used in the test setup, this value would be more than 3.5 billion cycles as determined by the prediction model.

6.2 Future Work

Further research into the use of coupons as a means of exploring the fatigue behaviour of FC should be looked upon, particularly in the design of tabs. The coupons did not exhibit the results that were expected, and it is unsure whether there is a fault within the samples or testing methodologies. The most probable cause as stated previously is the high stress loading on the tabs within the grips. Ever through this was justified throughout testing by reducing the pressure. Perhaps flexural fatigue tests on whole pultrusion sections would be a better option than coupons as this is a more accurate representation of the compression and tension forces in a bridge girder. Literature has also shown that the fatigue life, or fatigue testing is affected by the frequency and stress ratio at which testing is undertaken. Further testing into these effects would also be a valuable research topic.

Further research into testing large scale samples at high stresses should also be considered. If for example, the composite girder was put under similar stresses that the coupons were subject to (remembering that only tension forces were considered in coupon testing), would determine the accuracy of the coupon results. This would require shortening the girder so that higher stresses could be achieved. The pultruded FC samples seemed to be able to withstand heavy loads, however their performance in fatigue was not as satisfying, and therefore more studies into this field are needed.

Appendix A: Project Specification

University of Southern Queensland

FACULTY OF ENGINEERING AND SURVEYING

ENG4111/4112 Research Project
PROJECT SPECIFICATION

FOR: **Alan Owen TAYLOR**

TOPIC: INVESTIGATION INTO THE FATIGUE BEHAVIOUR OF PULTRUDED FIBRE COMPOSITES

SUPERVISORS: A/ Prof. Thiru Aravinthan
Michael Kemp, Wagners Composite Fibre Technologies Manufacturing Pty Ltd

SPONSORSHIP: Centre of Excellence in Engineered Fibre Composites
Wagners Composite Fibre Technologies Manufacturing Pty Ltd

PROJECT AIM: To investigate the fatigue behaviour of pultruded Fibre Reinforced Plastics (FRP) and by conducting small scale tests (coupon) to extrapolate the same results as for large scale beams.

PROGRAMME: (**Issue A, 11th March 2009**)

1. Research background information into the theory of fatigue life for steel, FRP, and existing fatigue studies.
2. Analysis of Wagners 9.7 m beam which has recently been fatigue tested at USQ facilities.
3. Develop a testing plan including placement of instrumentation, static and live loading of the coupons.
4. Fatigue test pultruded coupons for S-N curves.
5. Fatigue test pultruded coupons for beam design.
6. Fatigue test glue line coupons.
7. Develop S-N curves for pultruded FRP sections.
8. Determine whether or not small scale tests (coupon) can be used as a means of predicting the fatigue life of large scale beams.

As time permits:

9. Develop design guidelines considering fatigue behaviour.

AGREED:

_____ (Student) _____ , _____ (Supervisors)

___ / ___ / 20___ ___ / ___ / 20___ ___ / ___ / 20___

Examiner/Co-examiner: _____

Appendix B: Tensile Testing Raw Results

Specimen Number: 1
Tagged: False

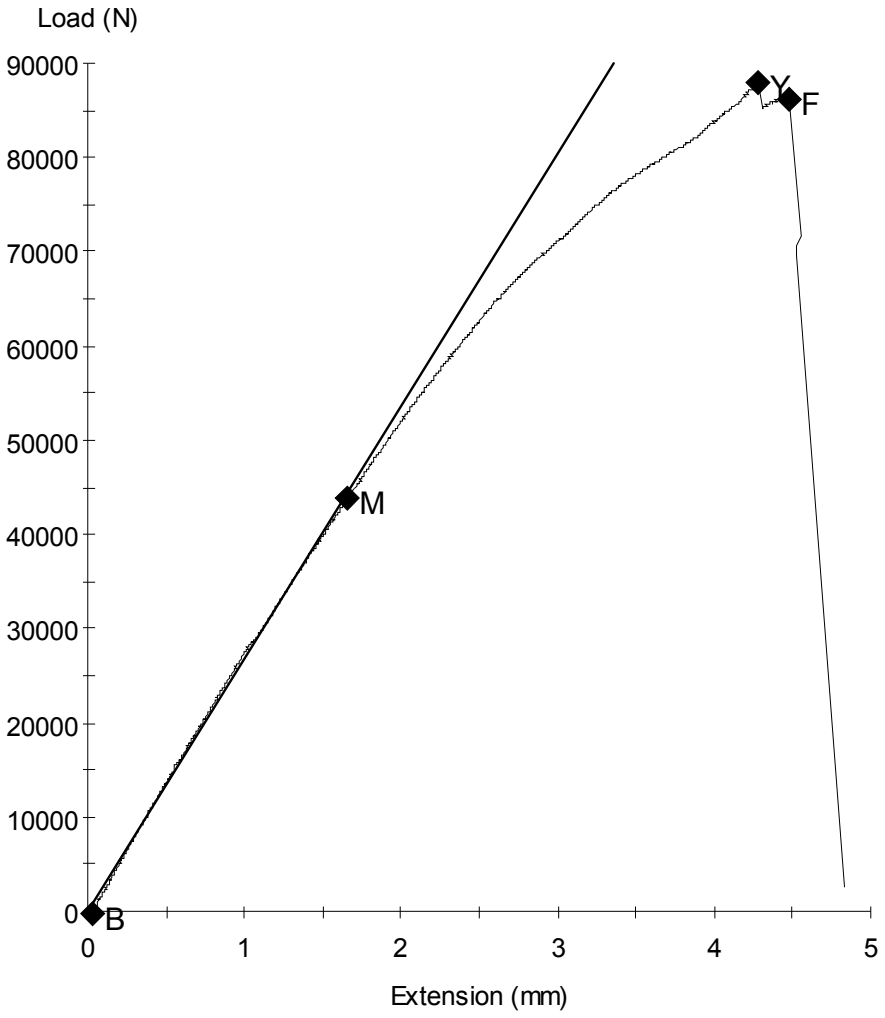

[2]

Specimen Results:

Name	Value	Units
Thickness	5.880	mm
Width	25.450	mm
Area	150	mm^2
Peak Load	87938	N
Peak Stress	587.64	MPa
Break Load	86276	N
Break Stress	576.54	MPa
Elongation At Break	4.479	mm
Stress At Offset Yield	292.233	MPa
Load At Offset Yield	43731.437	N

Specimen Number: 2
Tagged: False

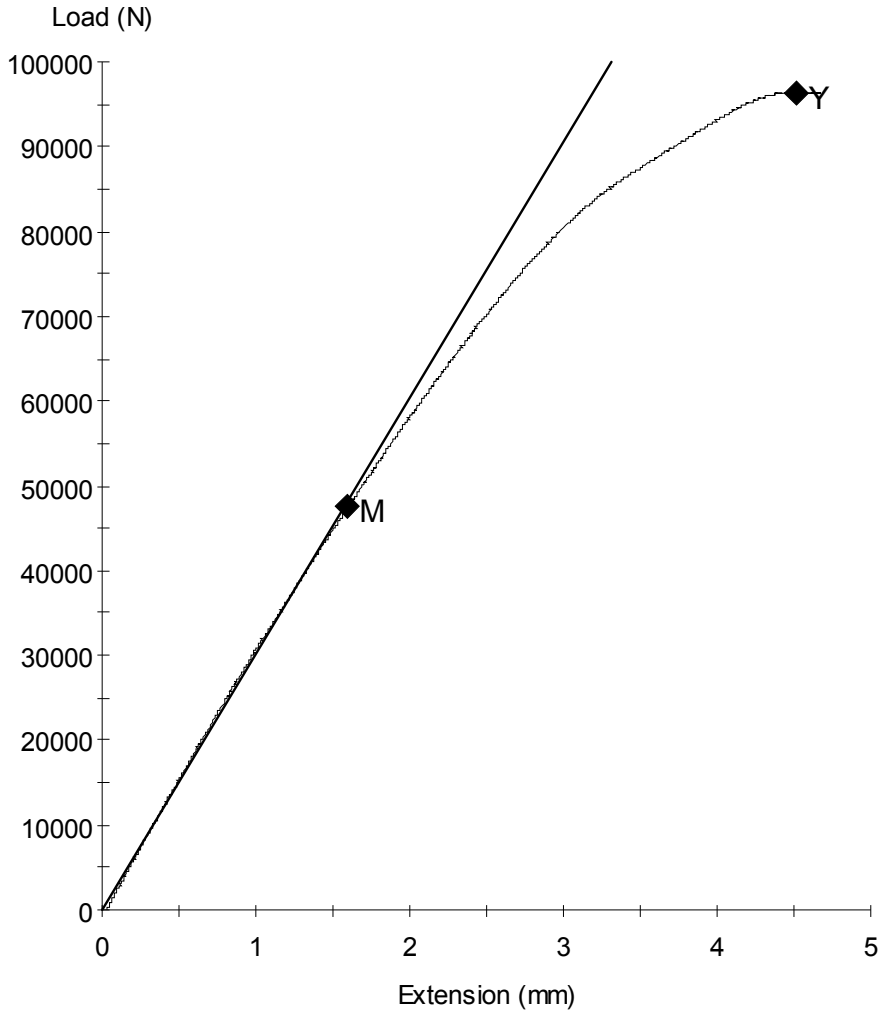

[3]

Specimen Results:

Name	Value	Units
Thickness	6.120	mm
Width	25.310	mm
Area	155	mm^2
Peak Load	96415	N
Peak Stress	622.45	MPa
Break Load	****	N
Break Stress	****	MPa
Elongation At Break	****	mm
Stress At Offset Yield	306.577	MPa
Load At Offset Yield	47487.960	N

Specimen Number: 3
Tagged: False

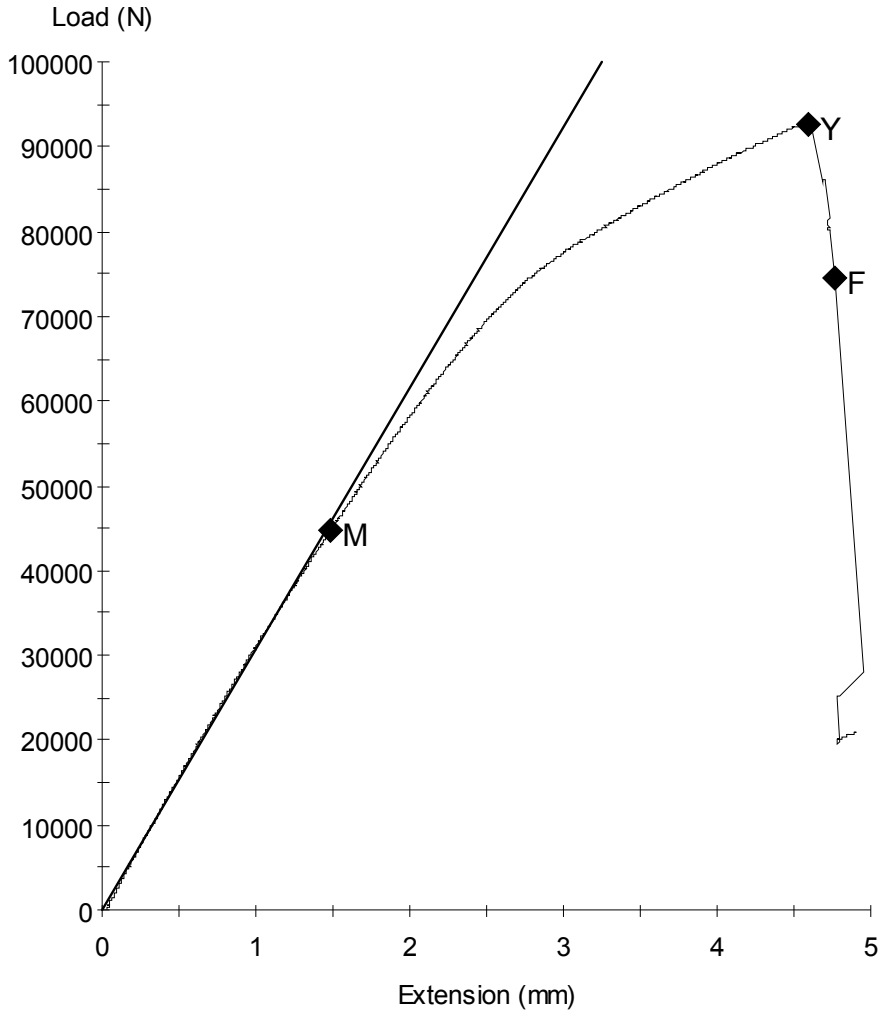

[4]

Specimen Results:

Name	Value	Units
Thickness	6.460	mm
Width	25.140	mm
Area	162	mm^2
Peak Load	92682	N
Peak Stress	570.69	MPa
Break Load	74563	N
Break Stress	459.12	MPa
Elongation At Break	4.759	mm
Stress At Offset Yield	276.431	MPa
Load At Offset Yield	44893.641	N

Specimen Number: 4
Tagged: False

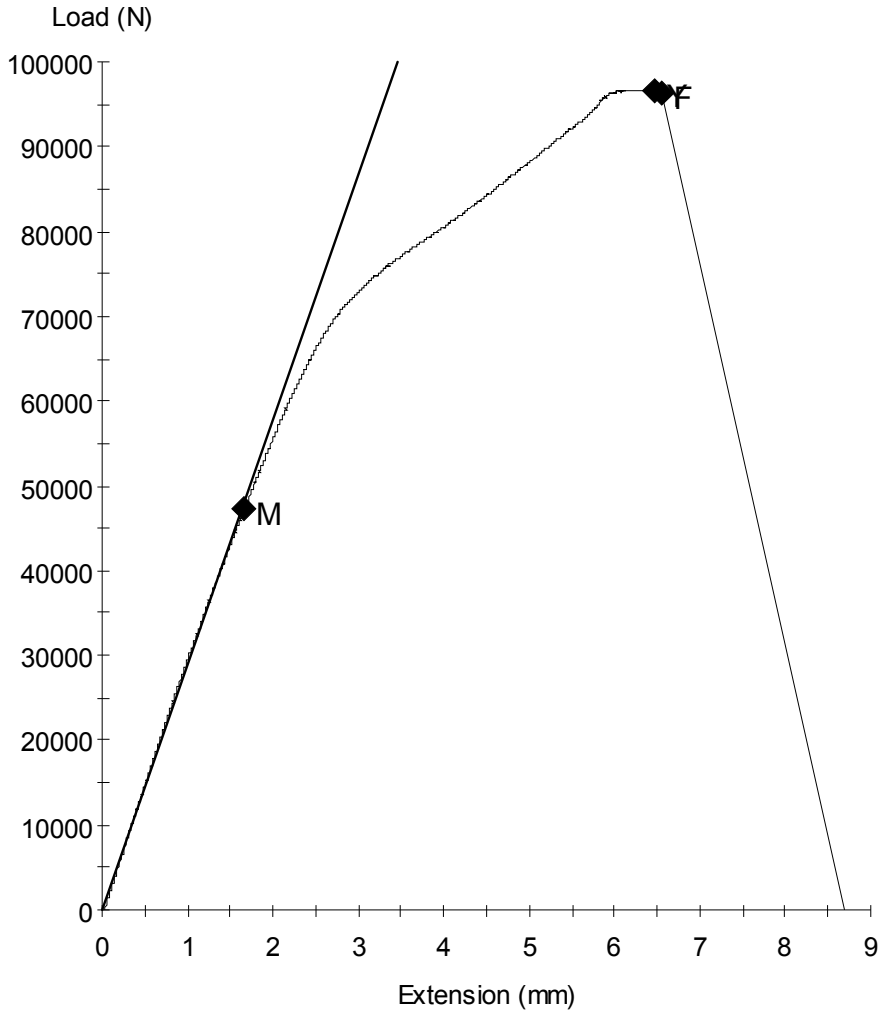

[5]

Specimen Results:

Name	Value	Units
Thickness	6.180	mm
Width	25.480	mm
Area	157	mm^2
Peak Load	96566	N
Peak Stress	613.25	MPa
Break Load	96292	N
Break Stress	611.51	MPa
Elongation At Break	6.542	mm
Stress At Offset Yield	301.025	MPa
Load At Offset Yield	47401.347	N

Specimen Number: 5
Tagged: False

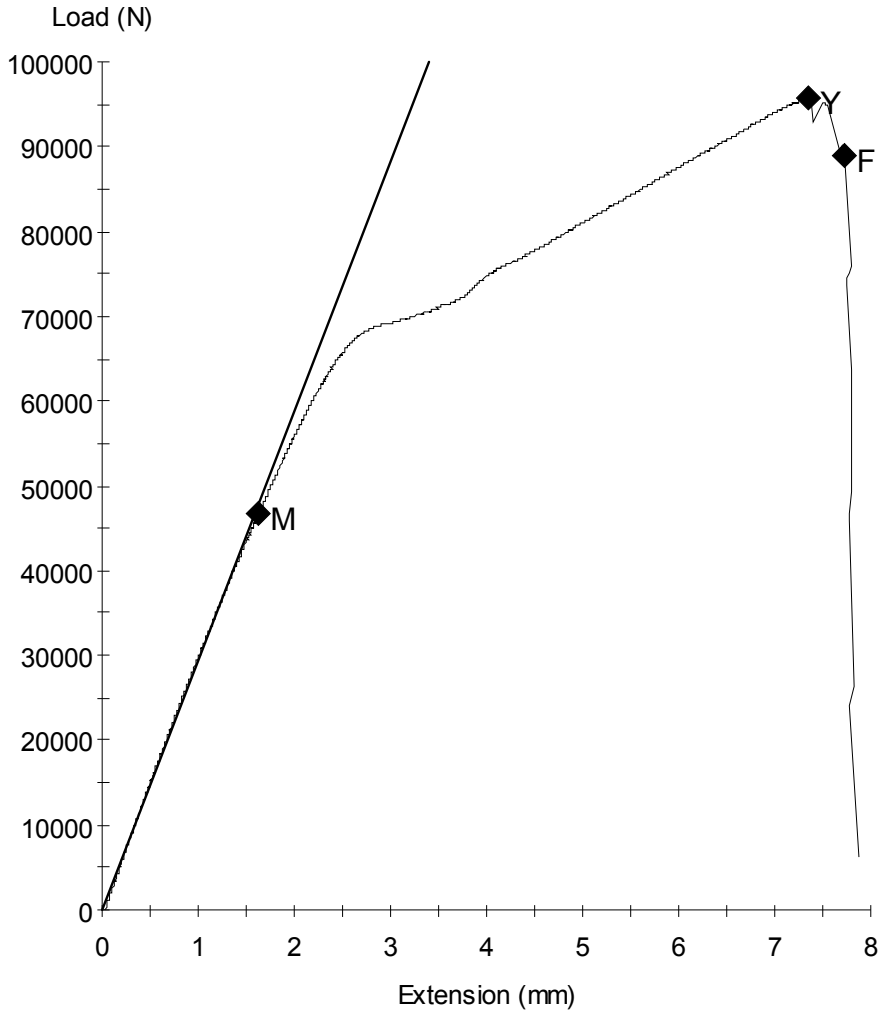

[6]

Specimen Results:

Name	Value	Units
Thickness	6.140	mm
Width	25.130	mm
Area	154	mm^2
Peak Load	95686	N
Peak Stress	620.14	MPa
Break Load	88853	N
Break Stress	575.85	MPa
Elongation At Break	7.715	mm
Stress At Offset Yield	302.246	MPa
Load At Offset Yield	46635.943	N

Appendix C: Dynamic Coupon Raw Results Sample

Cyclic Acquisition
Stored at: 1000 cycle
Points: 67

Axial Displacement mm	Axial Displacement Abs. Error mm	Time Sec	Axial Integer Count segments	Axial Load kN
1.1140678	6.76373E-07	338.03809	1999	29.93469
1.1039705	6.76373E-07	338.0481	1999	29.719841
1.0770444	6.76373E-07	338.05811	1999	28.991364
1.0332894	6.76373E-07	338.06812	1999	27.715689
0.96933985	6.76373E-07	338.07813	1999	25.990173
0.88856149	6.76373E-07	338.08813	1999	23.935667
0.80441737	6.76373E-07	338.09814	1999	21.629383
0.71690744	6.76373E-07	338.10815	1999	19.165319
0.61930025	6.76373E-07	338.11816	1999	16.627399
0.52505881	6.76373E-07	338.12817	1999	14.099551
0.43418312	6.76373E-07	338.13818	1999	11.63213
0.34667319	6.76373E-07	338.14819	1999	9.359417
0.26926059	6.76373E-07	338.1582	1999	7.3787651
0.2086768	6.76373E-07	338.16821	1999	5.7304606
0.16155608	6.76373E-07	338.17822	1999	4.4850001
0.13126419	6.76373E-07	338.18823	1999	3.6457412
0.11443536	6.76373E-07	338.19824	1999	3.2160406
0.10770383	6.76373E-07	338.20825	2000	3.162328
0.12453265	6.76373E-07	338.21826	2000	3.5651722
0.15819031	6.76373E-07	338.22827	2000	4.491714
0.2086768	6.76373E-07	338.23828	2000	5.8983121
0.27262634	6.76373E-07	338.24829	2000	7.6943264
0.35003898	6.76373E-07	338.2583	2000	9.8126163
0.43754888	6.76373E-07	338.26831	2000	12.165898
0.53179032	6.76373E-07	338.27832	2000	14.653462
0.622666	6.76373E-07	338.28833	2000	17.194738
0.71690744	6.76373E-07	338.29834	2000	19.702444
0.81451464	6.76373E-07	338.30835	2000	22.136295
0.895293	6.76373E-07	338.31836	2000	24.338511
0.96597409	6.76373E-07	338.32837	2000	26.218451
1.0265579	6.76373E-07	338.33838	2000	27.752617
1.0703129	6.76373E-07	338.34839	2000	28.894009

Appendix D: Composite Girder Raw Results Sample

Scan Session: "28-01-09 static
Start Time: 28/01/2009 8:23:37

ID	Seconds	[1] mm	[9] kN	[11] Strain	[12] Strain	[13] Strain	[14] Strain
1	11.4	0.012	-1.4163	-0.9626	0.482	0	0
2	11.5	0	-1.4163	-0.4813	0	-0.4817	0
3	11.6	0.024	-1.3909	0	0.9639	-0.4817	0
4	11.7	0.0359	-1.4163	0	1.4459	-0.9633	0
5	11.8	-0.012	-1.3909	-0.9626	0.9639	0	-0.4803
6	11.9	0	-1.4163	0	0.482	-0.4817	0
7	12	-0.024	-1.3909	0	0.9639	-1.445	0
8	12.1	0.024	-1.3909	0	0.482	-0.4817	0
9	12.2	-0.012	-1.3654	-0.4813	0	0.4817	-0.4803
10	12.3	0	-1.3909	0	0.9639	-0.4817	-0.4803
11	12.4	0	-1.3909	0.4813	0.9639	-0.4817	-0.4803
12	12.5	0	-1.34	-1.4438	0.482	-0.9633	0.9605
13	12.6	0.012	-1.4163	0	0.482	0	0
14	12.7	-0.012	-1.3909	0	0.482	0	0
15	12.8	0.012	-1.3909	-0.9626	0.9639	-0.4817	0.4803
16	12.9	0.012	-1.3909	0.4813	1.4459	-1.445	0.4803
17	13	-0.012	-1.34	0	0.9639	-0.9633	0
18	13.1	-0.012	-1.3654	0	0.482	-1.445	0.4803
19	13.2	0	-1.3909	-0.9626	0	-0.4817	0
20	13.3	-0.024	-1.3909	0	0.9639	-0.4817	0
21	13.4	0	-1.3909	-0.4813	0	-0.4817	-0.4803

Appendix E: Screen Shot of Dynamic Testing

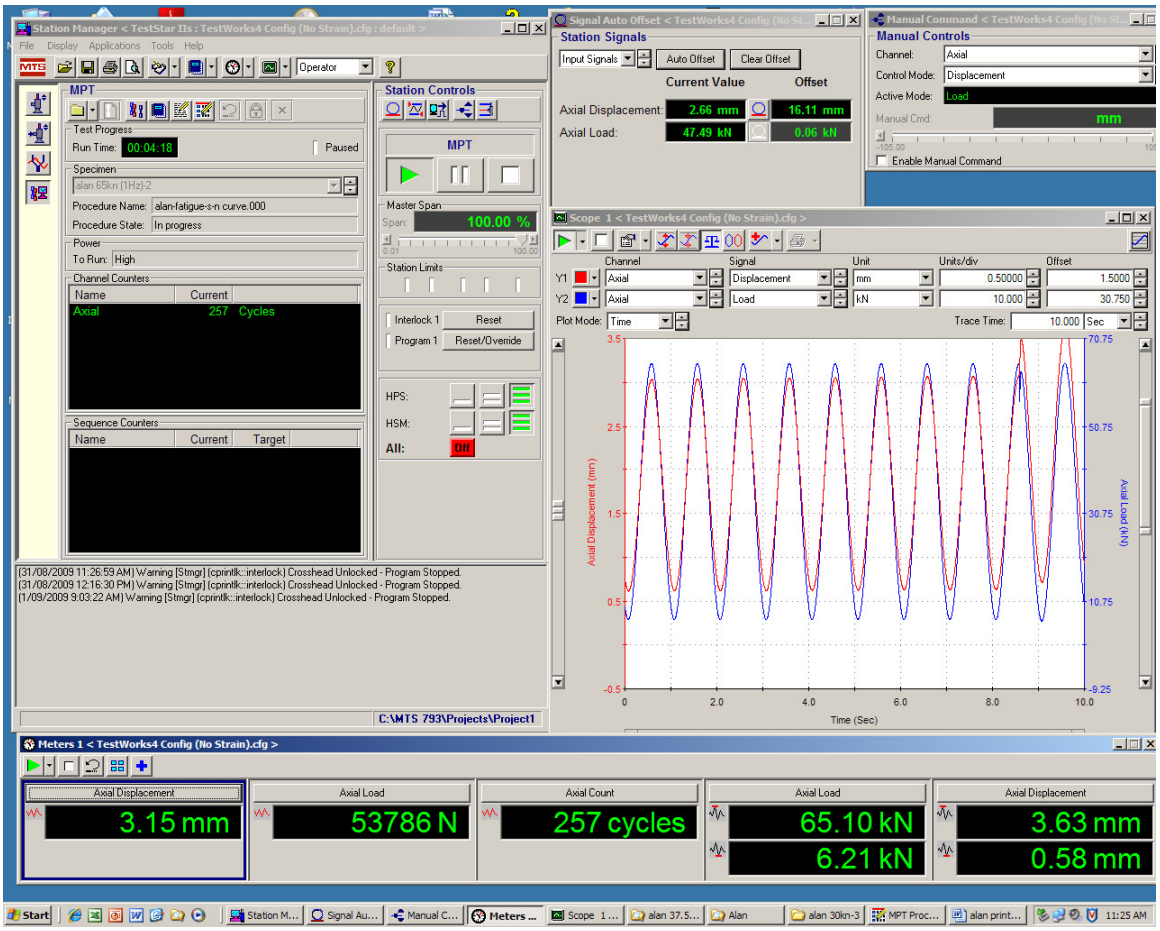

References

About.com, 10/13/1997, *The Pultrusion Process*, viewed 10th May 2009, Available Online < http://composite.about.com/library/weekly/aa101397.htm>

ASTM International, 2007, *ASTM D 3479/D 3479M,* viewed 10th May 2009, Available Online < http://www.astm.org/Standards/D3479.htm>

EPI Incorporated, 2008, *Metal Fatigue*, viewed 30th August 2009, Available Online <http://www.epi-eng.com/mechanical_engineering_basics/fatigue_in_metals.htm]>

J. A. Epaarachchi & P. D. Clausen, 2003, *'An empirical model for fatigue behaviour prediction of glass fibre-reinforced plastic composites for various stress ratios and test frequencies'*, Department of Mechanical Engineering, University of Newcastle, Australia.

Jolyn Louise Senne, 2000, '*Fatigue Life of Hybrid FRP Composite Beams'*, Master thesis, Virginia Polytechnic Institute and State University, Virginia.

Paul Grundy, 2003, '*Fatigue Design of Bridges in Australia'*, PhD thesis, Monash University, Australia.

Mohammed Shafeeq, 2006, *Effect of Environment on the Fatigue and Tensile Properties of Glass Fiber Reinforced Vinylester and Epoxy Thermosets*, Master of Science Thesis, library.kfupm.edu.sa/lib-downloads/A1S5333.pdf.

Robert K. Paasch, 1999, '*Fatigue Crack Modelling in Bridge Deck Connection Details'*, Report, Oregon State University, United States.

Standards Online, 2009, *AS4100, Section 11 - Fatigue,* viewed online 10th May 2009, Available Online <http://www.saiglobal.com>

R. I Stephens, A. Fatemi, R. R. Stephens, H. O. Fuchs, 2001, *'Metal Fatigue in Engineering'*, 2nd Edition, John Witey & Sons Inc.

R. O. Ritchie, Y. Murakami, 2009, '*Comprehensive Structural Integrity – Volume 4'*, 1st Edition, Elsevier Inc.

University of Southern Queensland 2009, *Polymer Matrix Materials for Civil and Structural Engineers,* Toowoomba, Australia.

University of Southern Queensland 2009, *Fibre Reinforcement for Composite Laminates,* Toowoomba, Australia.

University of Southern Queensland 2009, *Composite Material Behavior,* Toowoomba, Australia.

University of Southern Queensland 2009, *Durability of Fibre Composites,* Toowoomba, Australia.

Wagners Global, 2009, *Wagners Composite Fibre Technologies,* viewed 10th May 2009, Available Online < http://www.wagner.com.au/ >